

SI traceable characterization of nanomaterials by X-ray xpectrometry

Burkhard Beckhoff

Physikalisch-Technische Bundesanstalt
Abbestraße 2-12, 10587 Berlin, Germany

- analytical challenges for nanotechnologies
- reference-free x-ray spectrometry
- surface contamination and nanolayer characterization
- depth profiling at grazing incidence
- chemical speciation at buried interfaces
- operando speciation of bulk-type films
- high energy and spatial resolution spectrometry
- atomic fundamental parameter determinations

Analytical challenges for nanotechnologies

- dozens of **new nanoscaled materials** appear every month
- **technology R&D cycles** for new materials down to 4 months
- **need for correlation** of material properties with functionality
- **requirements** on sensitivity, selectivity and information depth
- most **analytical methodologies** rely on **reference materials** or calibration standards but there are only few at the nanoscale
- usage of **calibrated instrumentation** and knowledge on atomic data enables **reference-free techniques** such as SR based XRS

Challenges for nanotechnologies – nano-scaled reference materials

Nanoscaled Reference Materials (in line with ISO/TC 229 Nanotechnologies)

Reference materials are the key to guaranteeing reliability and correctness for results of chemical analyses and technical measurements.'

Categories:

- flatness
- film thickness
- single step , periodic step, step grating
- lateral X-Y-axis, 1-dim
- lateral X-Y-axis, +2-dim,
- critical dimensions
- 3-dimensional
- nanoobjects/nanoparticles/nanomaterial
- nanocrystallite materials
- porosity
- depth profiling resolution

Every month several tens new
nanoscaled materials appear.

The number of nanoscaled reference
materials is considerably lower.

Reference-free / first principles
based methodologies can address
this increasing gap.

Challenges for nanotechnologies – nano-scaled reference materials

Nanoscaled Reference

Reference materials and their use for results of chemical analysis

Categories:

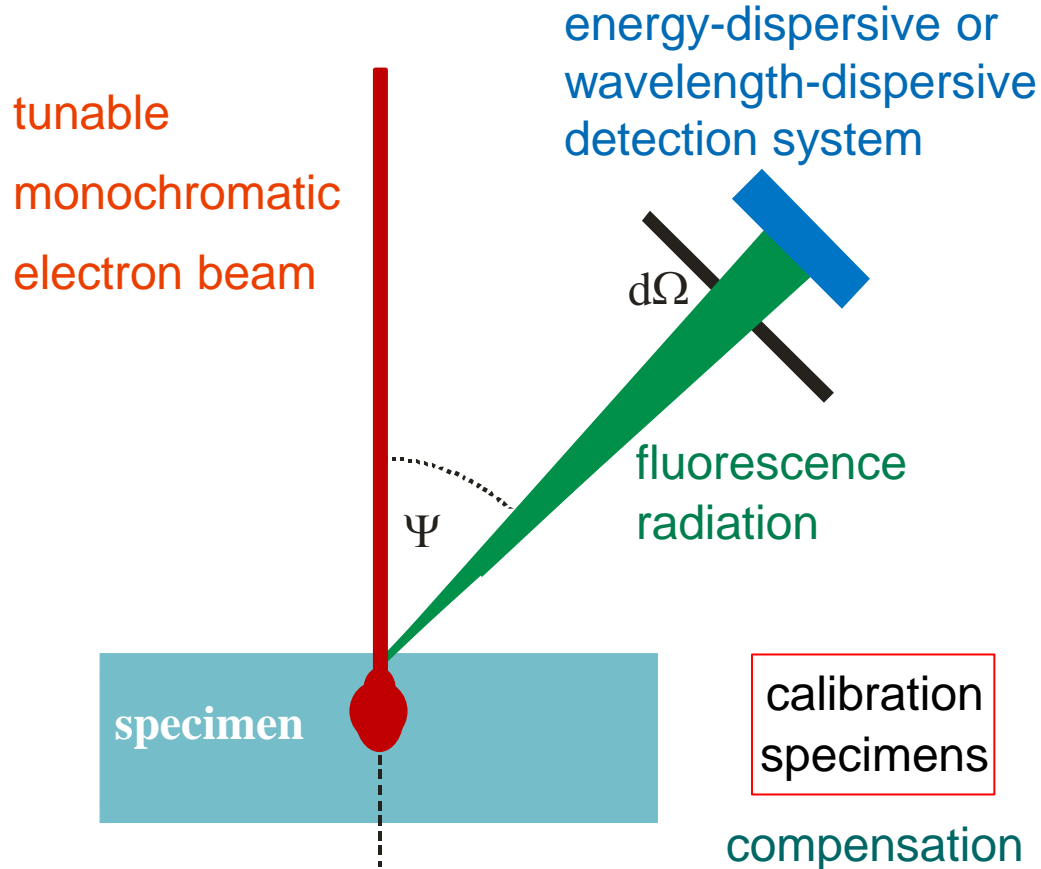
- flatness
- **film thickness**
- single step , periodic
- lateral X-Y-axis, 1-dim
- lateral X-Y-axis, +2-dim
- critical dimensions
- 3-dimensional
- **nanoobjects/nanoparticles**
- nanocrystallite materials
- porosity
- **depth profiling resolution**

Description	Certified values (nm)	RM name	RM type	RM no.
<u>Ti-Al multilayer 100/250 nm on 100Cr6 steel substrate</u>	100	BAM L-100	CRM	12
<u>Thickness standards, tantalum pentoxide film</u> Calibration of depth-resolving surface analysis	30	BCR-261	CRM	13
<u>Thickness standard, silicon dioxide film</u> NIST traceable	(2, 4.5, 7.5, 12, 25, 50, ...)	FTS	RM	3
<u>Thickness standards, silicon nitride film</u> NIST traceable	20	NFTS	RM	10
<u>Thickness standards, tungsten film</u> For best performance with sonar technology, an oxide layer 100 nm thick is added between the silicon substrate and the metal film, traceable to NIST	200	WFTS	RM	11
<u>GaAs/AlAs-superlattice</u> Calibration of depth resolution	23	CRM 5201-a	CRM	32
<u>SiO2/Si multilayer film reference material</u> Consist of five layers with SiO2 and Si grown using r.f. magnetron sputtering method on aSi substrate. The thickness of each layer is certified in units of length via X-ray reflectometry, control the precision of analysis and to regulate measurement condition in depth profile analysis by ion	20	NMIJ CRM 5202-a	CRM	54
<u>GaAs/AlAs super lattice</u> The CRM has six-layer-structure and the certified values for the thickness from the second to sixth layer are given; control the precision of analysis and to regulate measurement condition in depth profile analysis by ion sputtering	9,51	NMIJ CRM 5203-a	CRM	55
<u>Ultrathin silicon dioxide film</u> 3.49 nm (0.19 nm); control the precision of analysis and to regulate measurement condition in depth profile analysis by ion sputtering	3,49	NMIJ CRM 5204-a	CRM	56

X-ray emission spectrometry:

electron beam excitation - X-ray beam excitation

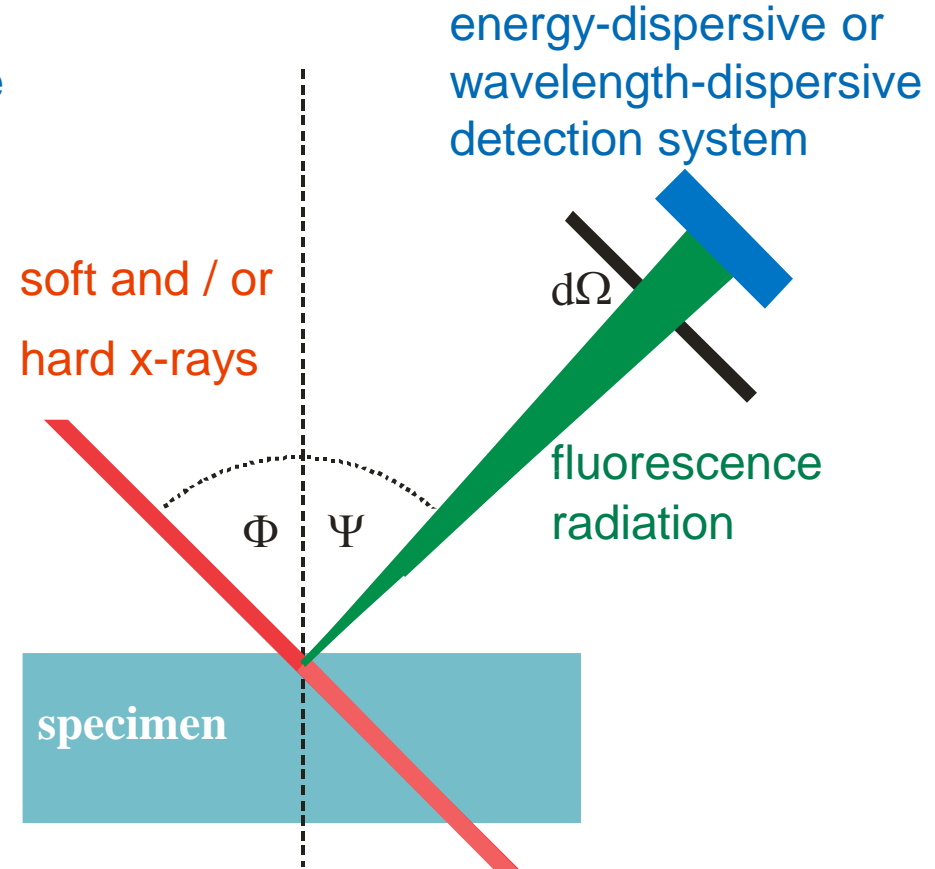
EDS



high sensitivity for low Z
small beam profiles
small penetration depth

calibration specimens
compensation for missing knowledge

XRS



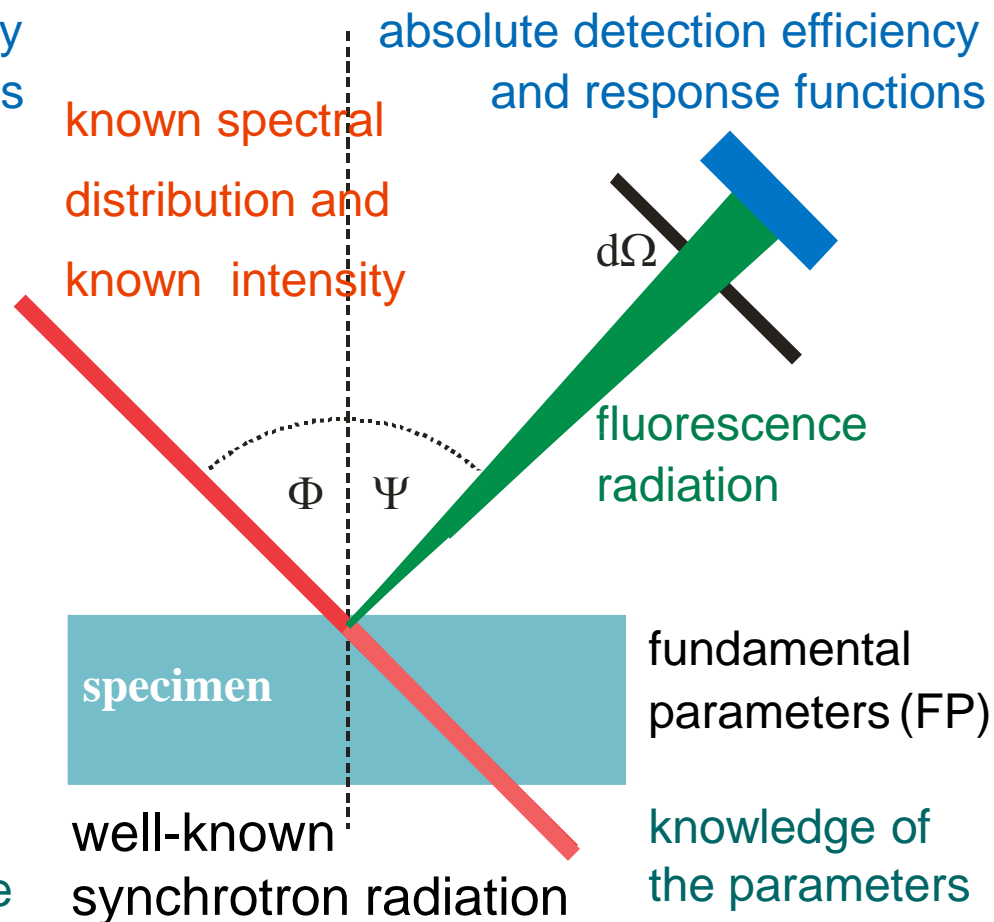
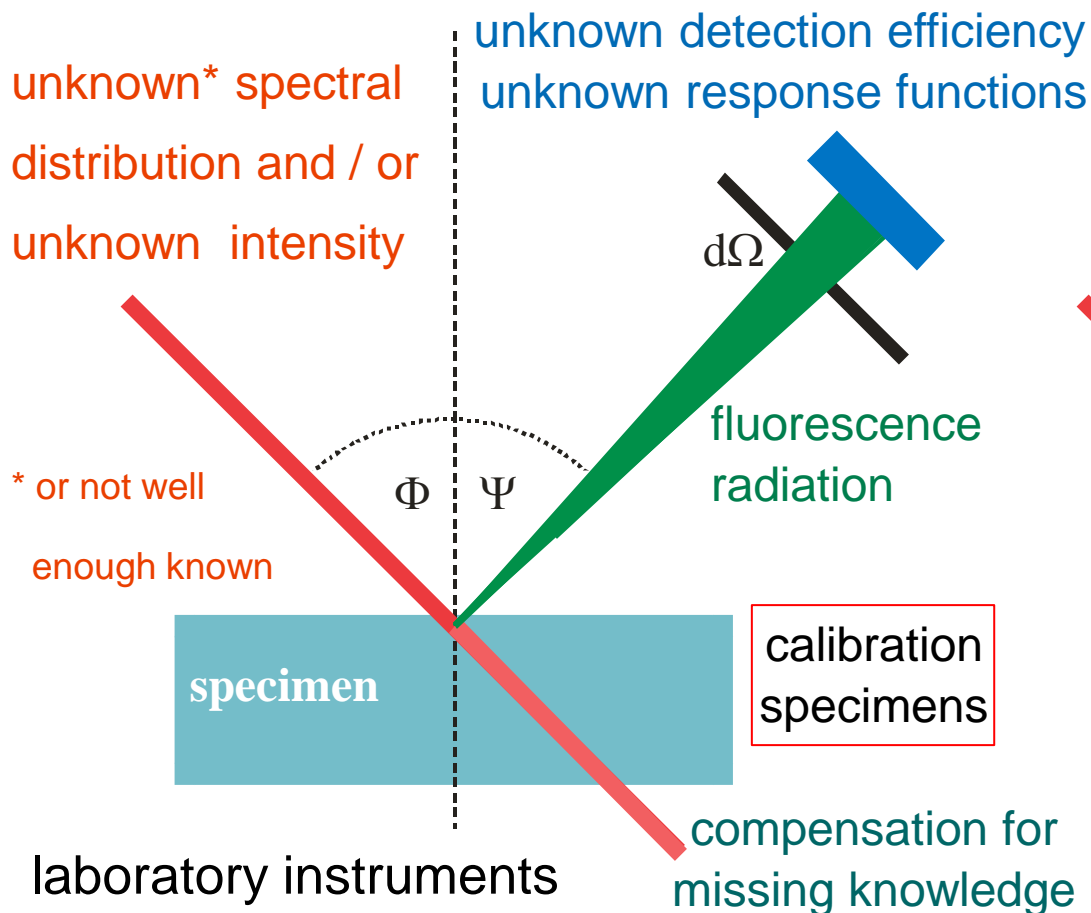
high sensitivity for medium to high Z
moderate beam profiles
moderate to large penetration depth

X-Ray Fluorescence (XRF) analysis:

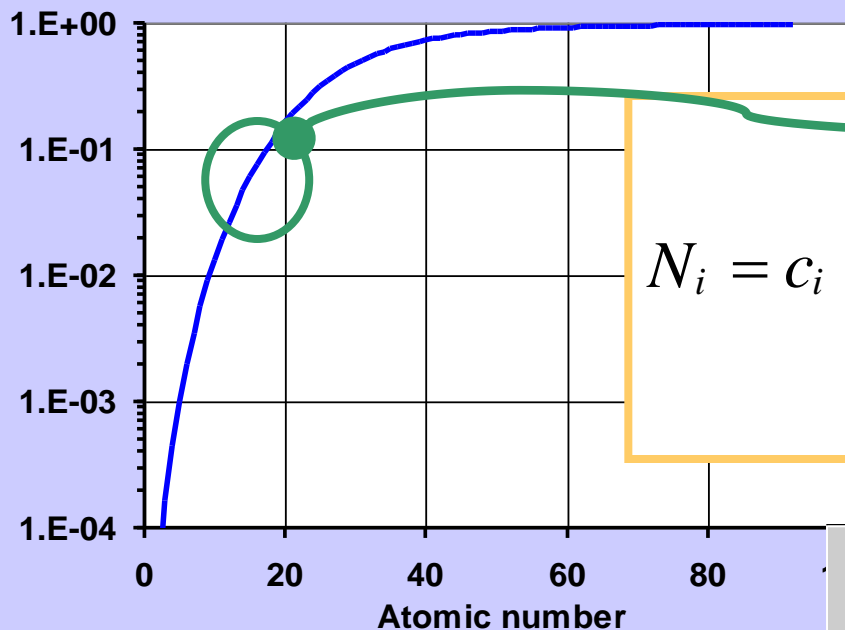
reference material based - reference-free approaches

conventional technique based on calibration or reference materials

reference-free technique based on calibrated instrumentation and FPs

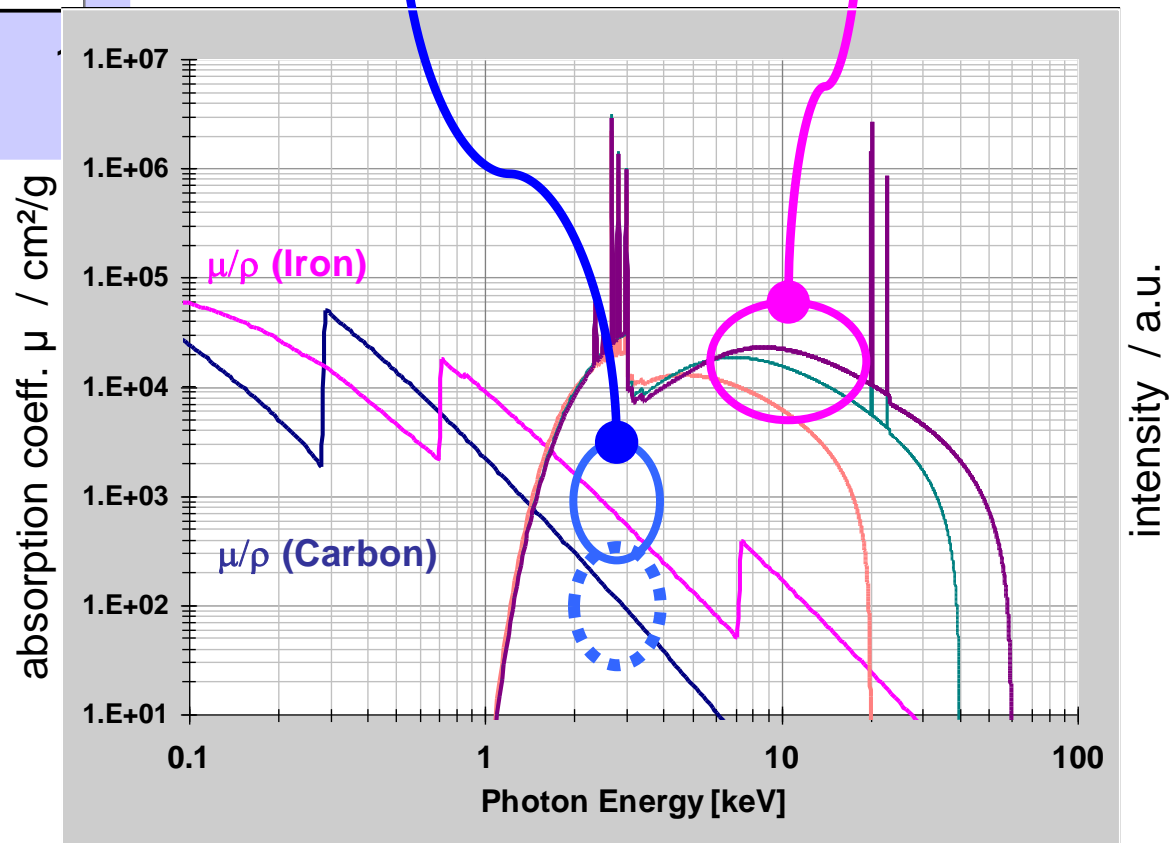


fluorescence yield



$$N_i = c_i \cdot G \cdot \int_E \frac{\frac{S-1}{S} \cdot p_i \cdot \omega_i \cdot \tau_i(E)}{\frac{\mu(E)}{\sin \psi_1} + \frac{\mu(i)}{\sin \psi_2}} \cdot N_0(E) \cdot dE$$

Fundamental parameter approach in XRF analysis



Typical XRF quantification variants:

α - coefficients

- empirical coefficients
- interpolation regime for main matrix elements or traces in constant matrices
- extrapolation restricted

reference material based

(chemical traceability)

- pre-calibration of instrumentation e.g. by thin *standards*
- additional calibration by reference materials for specific *applications*
- interpolation by good knowledge of FP data

reference-free methodology

(physical traceability to SI system)

- good knowledge on both instrumental and fundamental parameters (FP)
- increasing relevance for complex sample systems, e.g. nano-scaled specimens or operando studies
- reason: lack of appropriate reference materials or calibration standards

→ *Relevant contribution of knowledge on FP on the uncertainty of the analytical results*

Synchrotron radiation based x-ray spectrometry

XRS excitation channel:

well-known spectral distribution
and a well-known radiant power

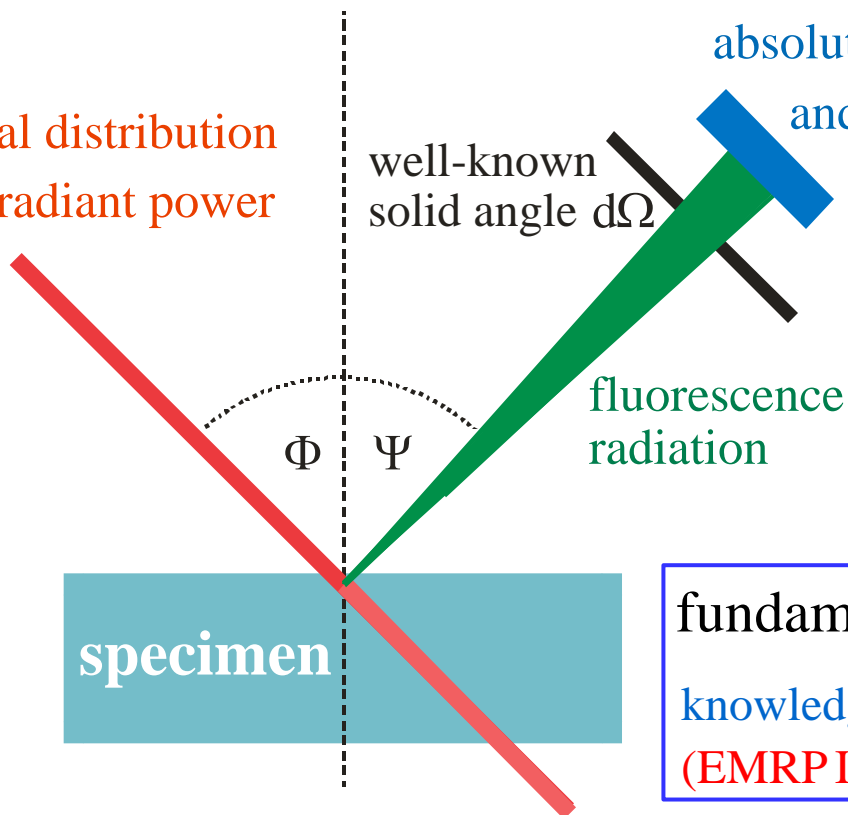
XRS detection channel:

absolute detection efficiency
and response functions

derived from
x-ray radiometry

PTB capabilities:

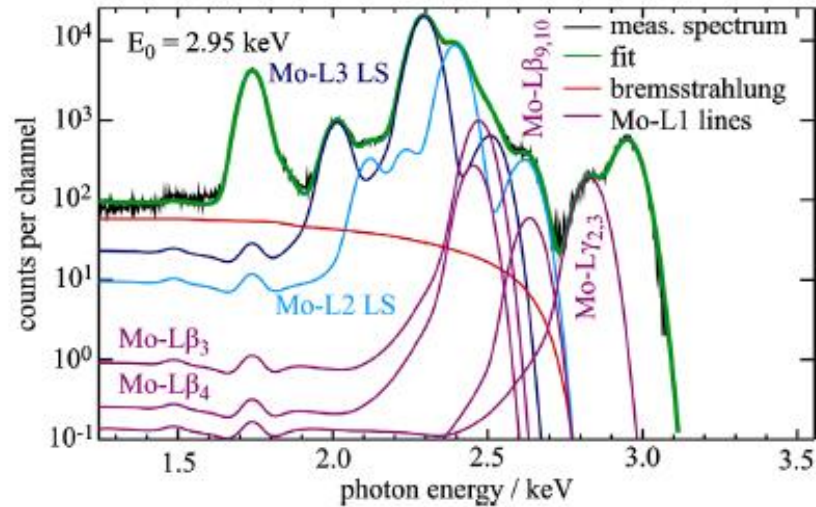
- characterized beamlines
- calibrated photodiodes
- calibrated diaphragms
- calibrated Si(Li) detectors



fundamental parameters
knowledge of atomic parameters
(EMRP IND07, NEW01, ENG53)

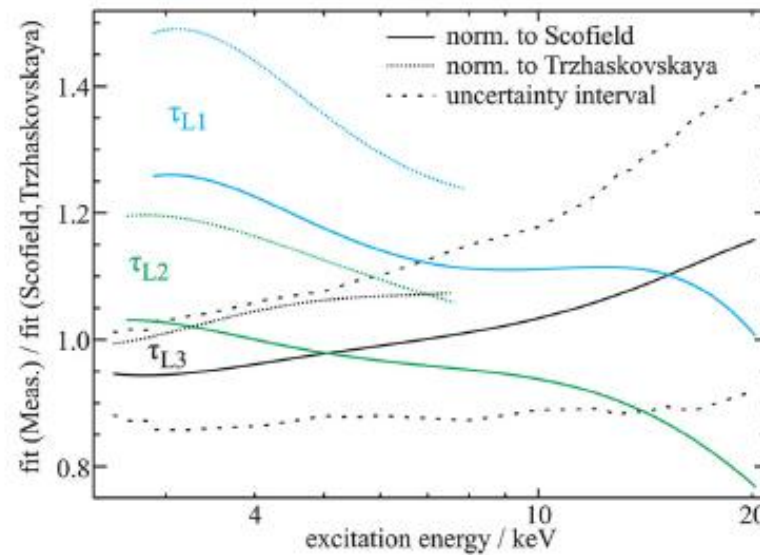
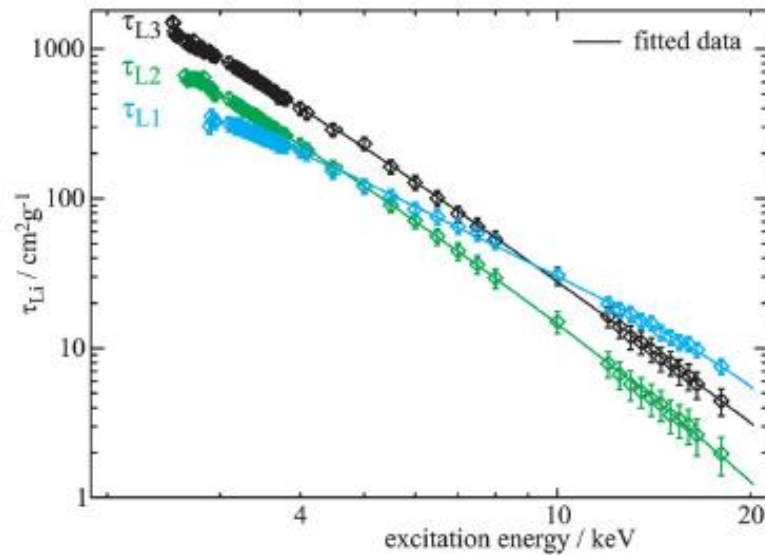
transmission measurements
absorption correction factors

Determination of L-shell photoionization cross sections



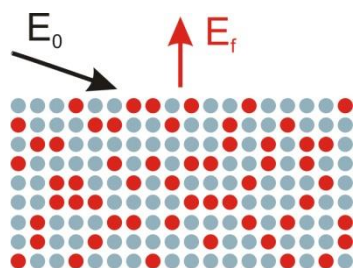
Response function based deconvolution of a Mo layer XRF spectrum for each L-shell.

Experimentally determined PCS for the Mo-L subshells and the comparison to calculated data.



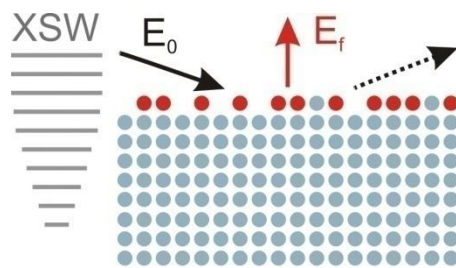
Tuning the analytical sensitivity and information depth by means of appropriate operational parameters

excitation conditions



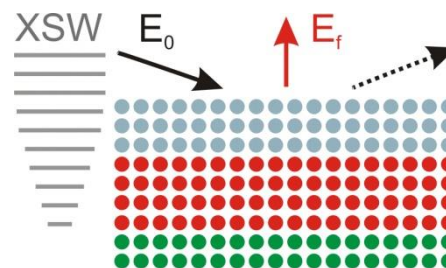
concentration

total-reflection



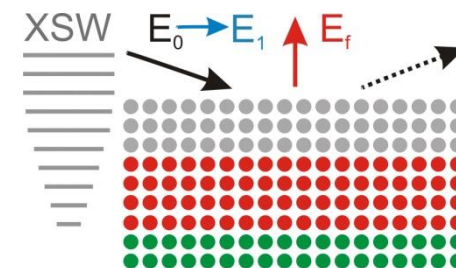
contamination

tunable incident angle



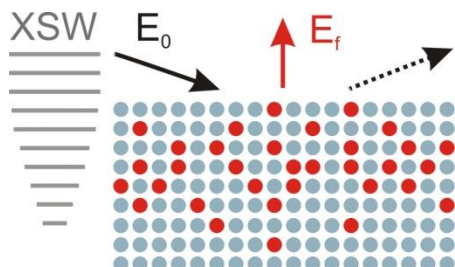
nanolayer

tunable photon energy



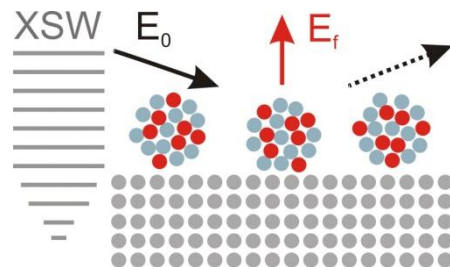
nanolayer speciation

tunable incident angle



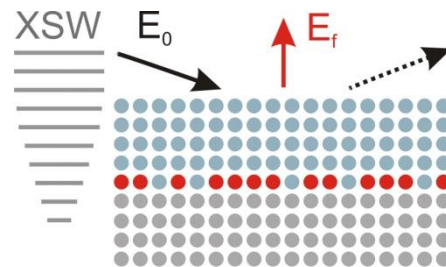
depth profile

total-reflection



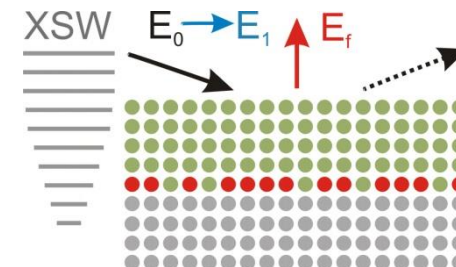
nanoparticles

tunable incident angle



interface

tunable photon energy



interface speciation

E_0 = photon energy of excitation radiation

E_1 = photon energy above absorption edge

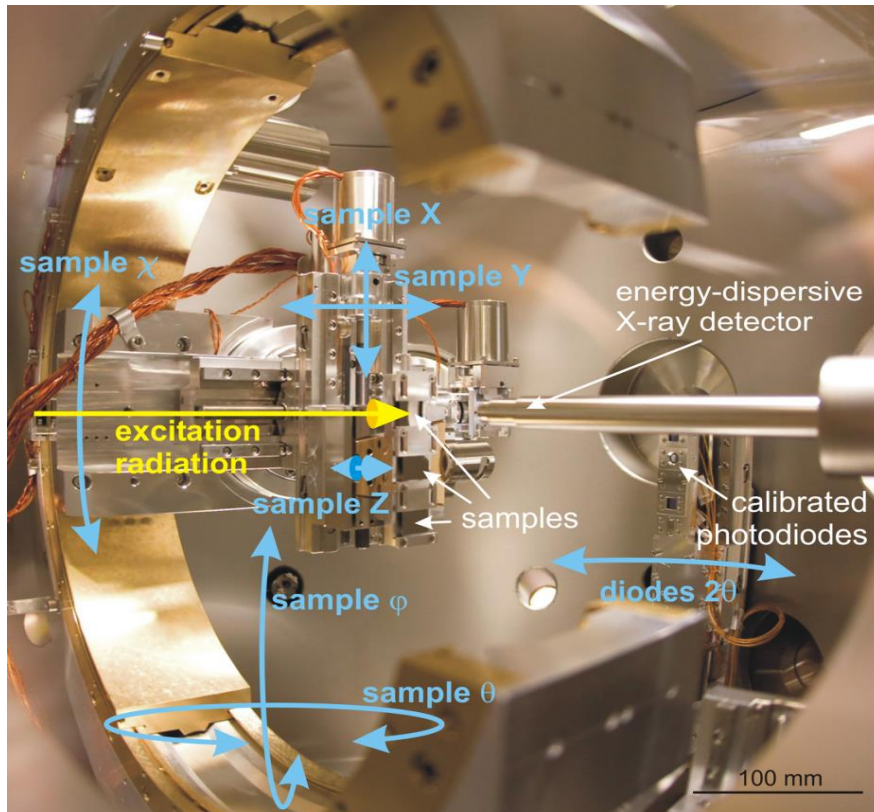
E_f = photon energy of fluorescence radiation

XSW = X-ray Standing Wave field

J. Anal. At. Spectrom. **23**, 845 (2008)

Novel XRS instrumentation for advanced materials characterizations with synchrotron radiation

PTB XRS instrumentation at BESSY



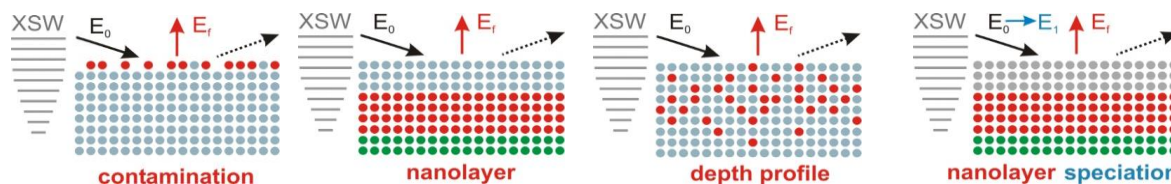
9-axis manipulator and chamber ensuring

- the entire TXRF, GIXRF and XRF regime
- polarization-dependent speciation by XAFS
- combined GIXRF and XRR investigations
- movable aperture system for reference-free XRF and atomic FP determinations

→ μm - and nm -beam forming optics options

Transfer of modified instrumentation to

- TU Berlin for a **laboratory plasma source**
- LNE/CEA-LNHB for **SOLEIL storage ring**
- IAEA (UN) for **ELETTRA storage ring**



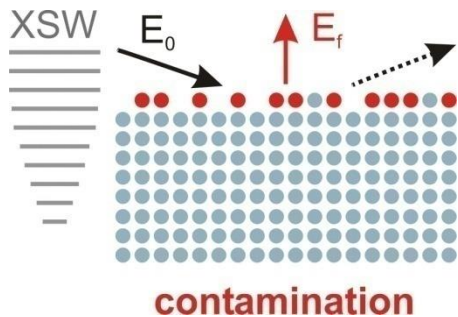
Rev. Sci. Instrum. **84**, 045106 (2013)

AIP **1741**, 030011 (2016)

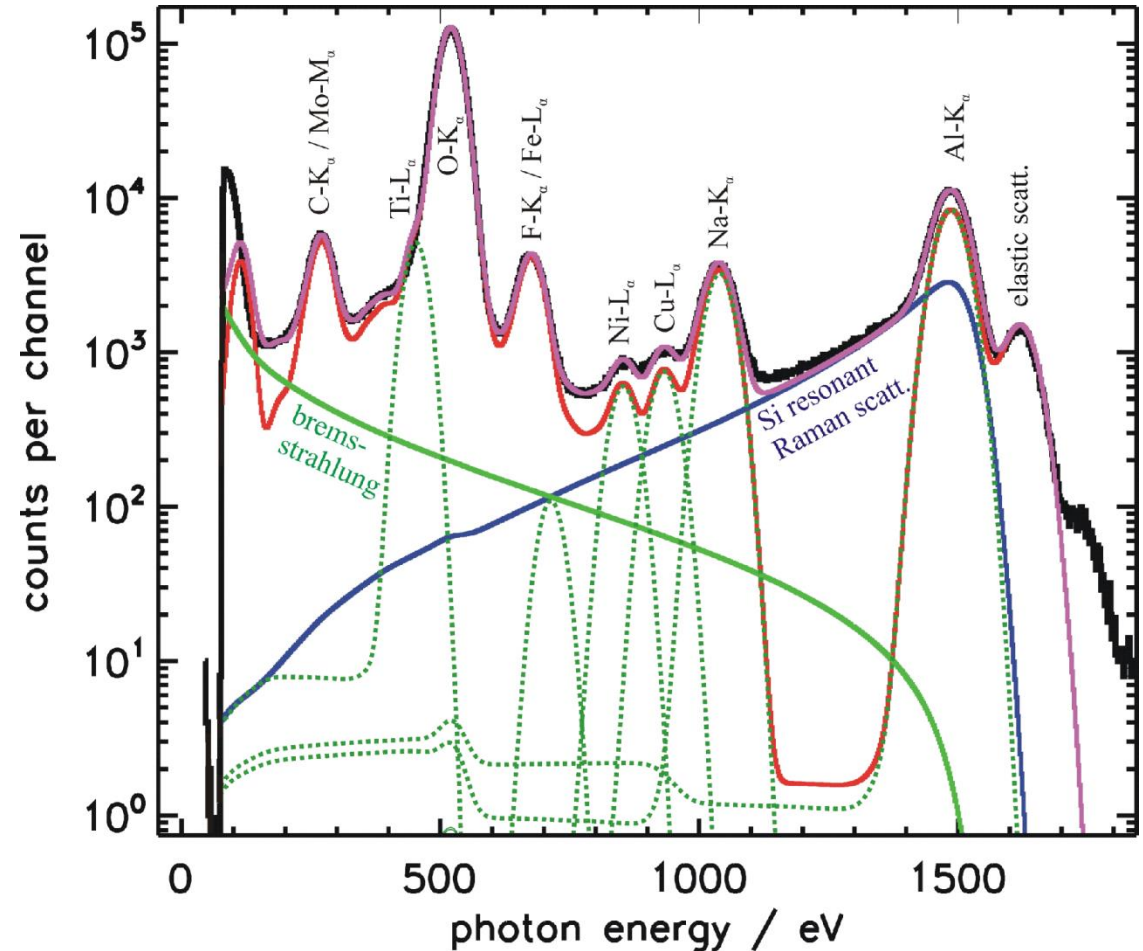
Reference-free quantitation in TXRF analysis on Si wafers

TXRF spectra deconvolution including SDD detector response functions, RRS, and bremsstrahlung contributions.

reference-free TXRF quantitation: known incident flux, detector efficiency and solid angle.



spin-coated wafer with 10^{12} cm⁻² of various transition metals



Reference-free quantitation in SR-TXRF analysis

mass deposition m_i / F_I of the element i with unit area F_I

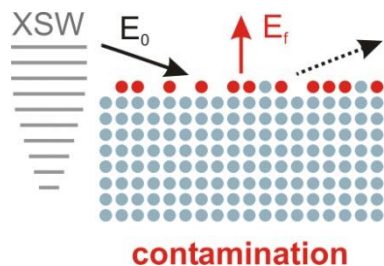
$$\frac{m_i}{F_I} = \frac{-1}{\mu_{tot,i}} \ln \left\{ 1 - \frac{P_i}{P_{0,Wsurf} \tau_{i,E_0} Q \frac{\Omega_{det}}{4\pi} \frac{1}{\sin \psi_{in}} \frac{1}{\mu_{tot,i}}} \right\}$$

E_0 photon energy of the incident (excitation) radiation

$P_0 = S_0 / \sigma_{diode,E_0}$ radiant power of the incident radiation

S_0 signal of the photodiode measuring the incident radiation

σ_{diode,E_0} spectral responsivity of the photodiode



Reference-free quantitation in SR-TXRF analysis

mass deposition m_i / F_I of the element i with unit area F_I

$$\frac{m_i}{F_I} = \frac{-1}{\mu_{tot,i}} \ln \left\{ 1 - \frac{P_i}{P_{0,Wsurf} \tau_{i,E_0} Q \frac{\Omega_{det}}{4\pi} \frac{1}{\sin \psi_{in}} \frac{1}{\mu_{tot,i}}} \right\}$$

I_{Wsurf}

relative intensity of the X-ray standing wave field¹ at the wafer surface

$$P_{0,Wsurf} = P_0 I_{Wsurf}$$

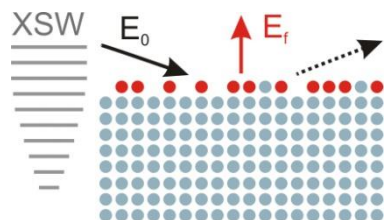
¹ software package IMD: D. Windt, Computers in Physics **12**, 360-370 (1998)

ψ_{in}

angle of incidence with respect to the wafer surface

E_i

photon energy of the fluorescence line l of the element i



contamination

Reference-free quantitation in SR-TXRF analysis

mass deposition m_i / F_I of the element i with unit area F_I

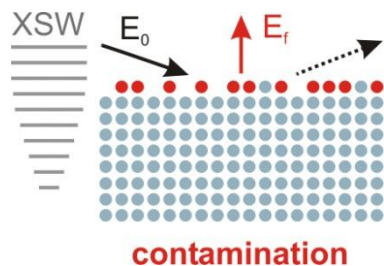
$$\frac{m_i}{F_I} = \frac{-1}{\mu_{tot,i}} \ln \left\{ 1 - \frac{P_i}{P_{0,Wsurf} \tau_{i,E_0} Q \frac{\Omega_{det}}{4\pi} \frac{1}{\sin \psi_{in}} \frac{1}{\mu_{tot,i}}} \right\}$$

R_i detected count rate of the fluorescence line l of the element i

ε_{det,E_i} detection efficiency of the Si(Li) detector at the photon energy E_i

$$P_i = R_i / \varepsilon_{det,i}$$

Ω_{det} effective solid angle of detection



Reference-free quantitation in SR-TXRF analysis

mass deposition m_i / F_I of the element i with unit area F_I

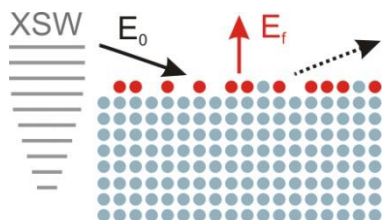
$$\frac{m_i}{F_I} = \frac{-1}{\mu_{tot,i}} \ln \left\{ 1 - \frac{P_i}{P_{0,Wsurf} \tau_{i,E_0} Q \frac{\Omega_{det}}{4\pi} \frac{1}{\sin \psi_{in}} \frac{1}{\mu_{tot,i}}} \right\}$$

ψ_{out} angle of observation which equals 90° in a typical TXRF geometry

τ_{i,E_0} photo electric cross section of the element i at the photon energy

$\mu_{i,E}$ absorption cross section of the element i at the photon energy E

$$\mu_{tot,i} = \mu_{i,E_0} / \sin \psi_{in} + \mu_{i,E_i} / \sin \psi_{out}$$



contamination

Reference-free quantitation in SR-TXRF analysis

mass deposition m_i / F_I of the element i with unit area F_I

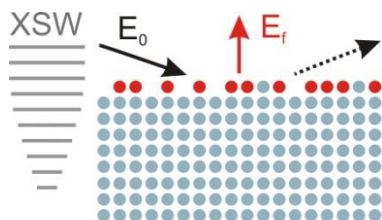
$$\frac{m_i}{F_I} = \frac{-1}{\mu_{tot,i}} \ln \left\{ 1 - \frac{P_i}{P_{0,Wsurf} \tau_{i,E_0} Q \frac{\Omega_{det}}{4\pi} \frac{1}{\sin \psi_{in}} \frac{1}{\mu_{tot,i}}} \right\}$$

ω_{Xi} fluorescence yield of the absorption edge Xi (of the element i)

$g_{l,Xi}$ transition probability of the fluorescence line l belonging to Xi

j_{Xi} jump ratio at the absorption edge Xi

$$Q = \omega_{Xi} g_{l,Xi} (j_{Xi} - 1) / j_{Xi}$$



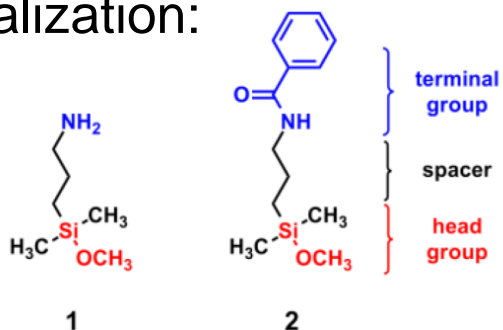
contamination

Analysis of contamination on novel materials
(Ge, SOI, InGaAs, ...) or of nanolayered
systems (buried interfaces – photovoltaics)

→ calculation of the x-ray standing wave field

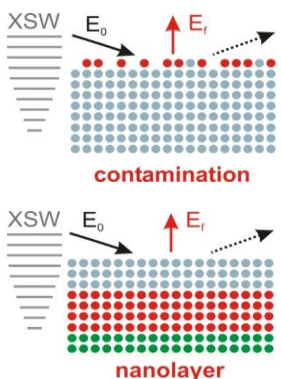
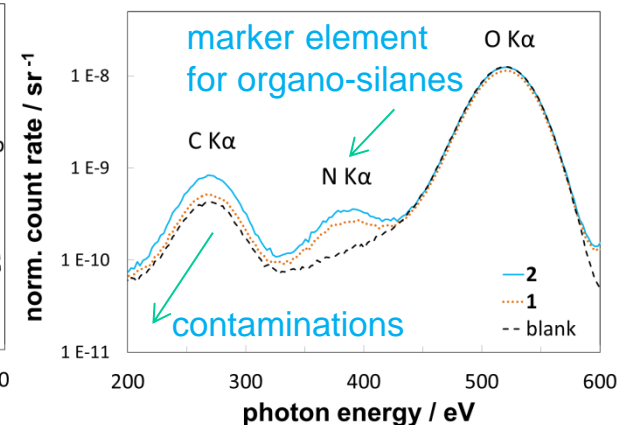
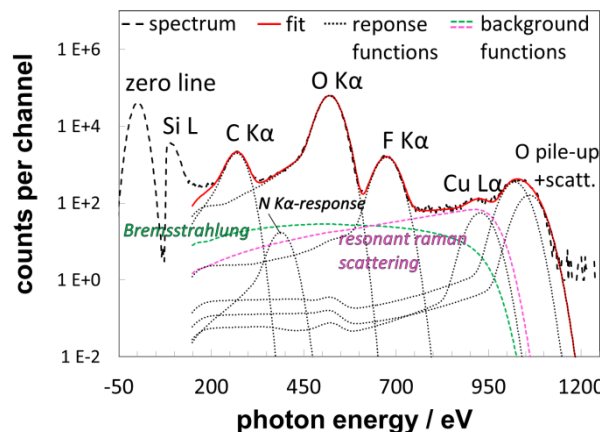
Traceable quantification of functionalized surfaces by means of reference-free TXRF analysis

- Single organo-silanes for surface functionalization:



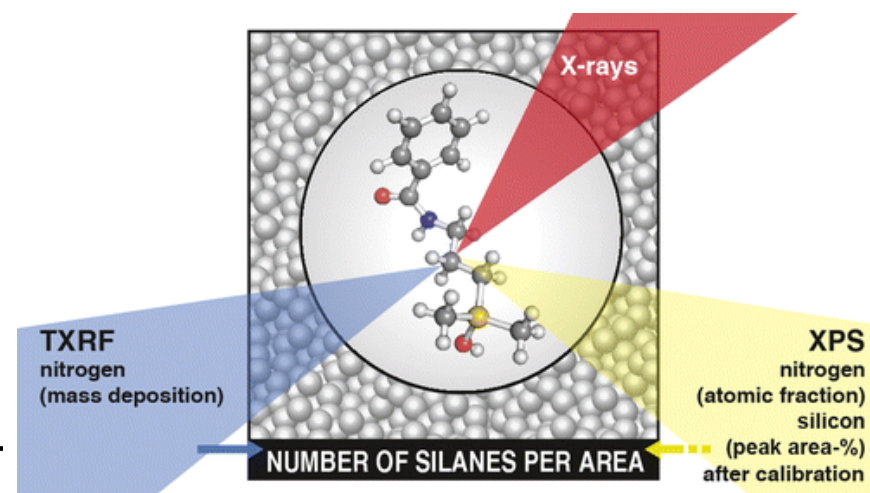
- molecular surface density as revealed by reference-free TXRF
- traceable quantification based on specific elements as **marker** (nitrogen)

Spectral deconvolution:



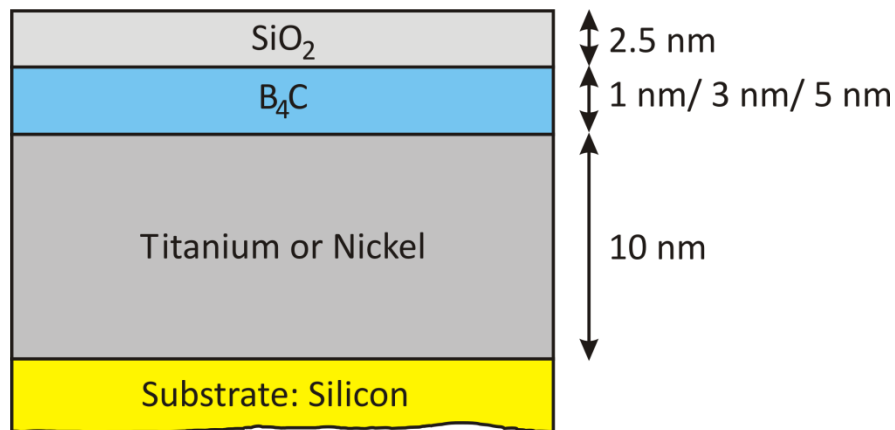
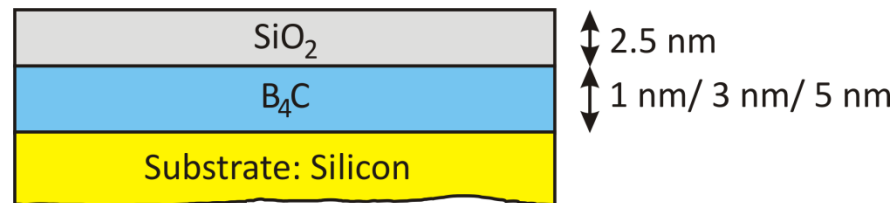
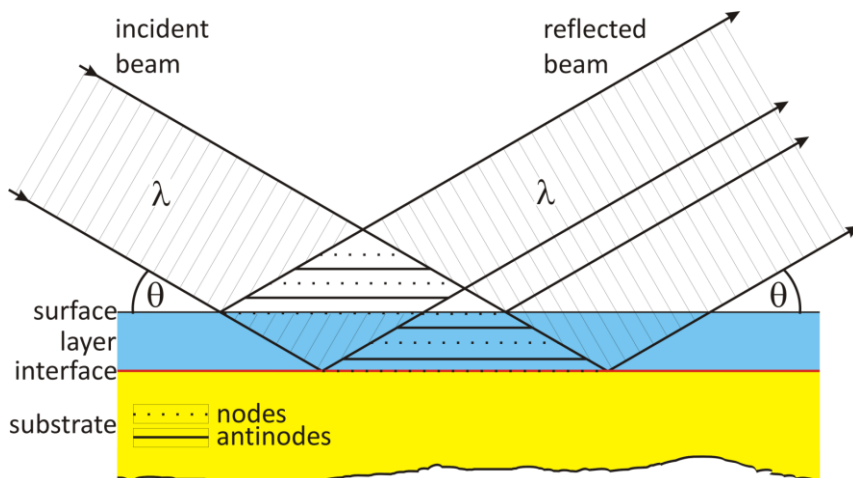
layer	TXRF		
	nitrogen $\left[\frac{ng}{cm}\right]$	silane areic density $\left[\frac{molecules}{nm^2}\right]$	thickness ¹ [nm]
1	5.9±1.8	2.5±0.8	0.6±0.2
2	8.9±2.7	3.8±1.1	1.4±0.5

C. Streeck, A. Nutsch



Reference-free XRF and grazing-incidence XRF of buried nanolayers - layer composition and thickness

X-ray standing wave field (XSW)

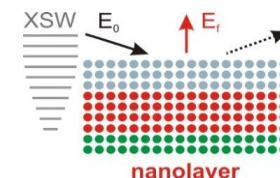


design of samples: total-reflection of the incident beam at silicon or at the metal

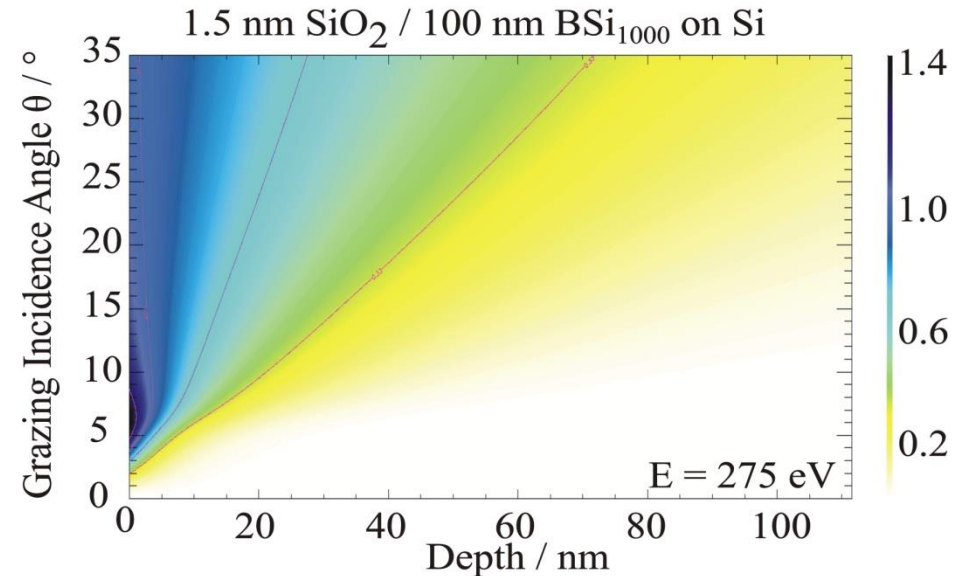
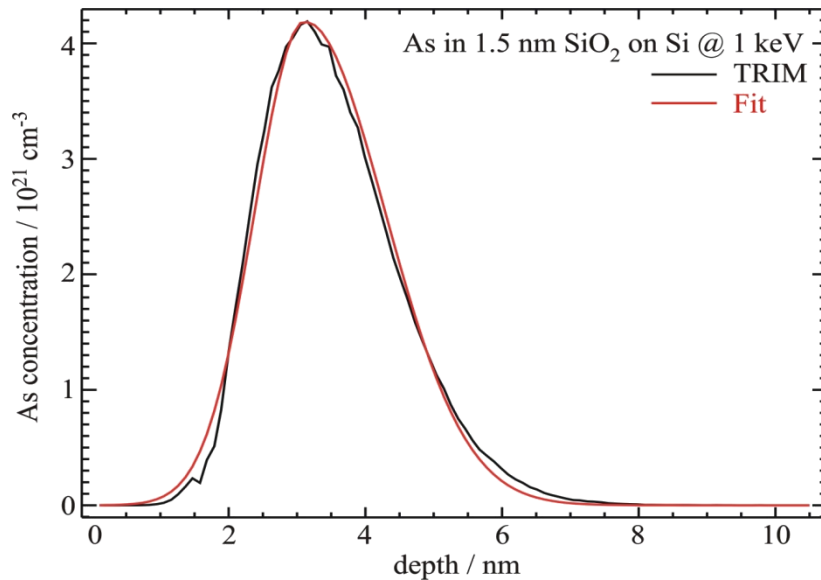
→ occurrence of the XSW in boron carbide layer

objective: determination of the boron carbide layer composition and thickness

→ comparison of XRF and GIXRF quantification



GIXRF analysis of B and As implantation profiles

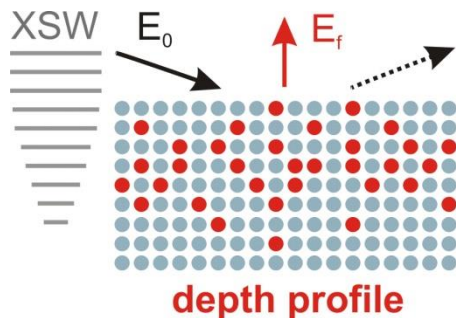


fundamental and instrumental parameters

depth distribution of the implant

X-ray Standing Wave field distribution

absorption term



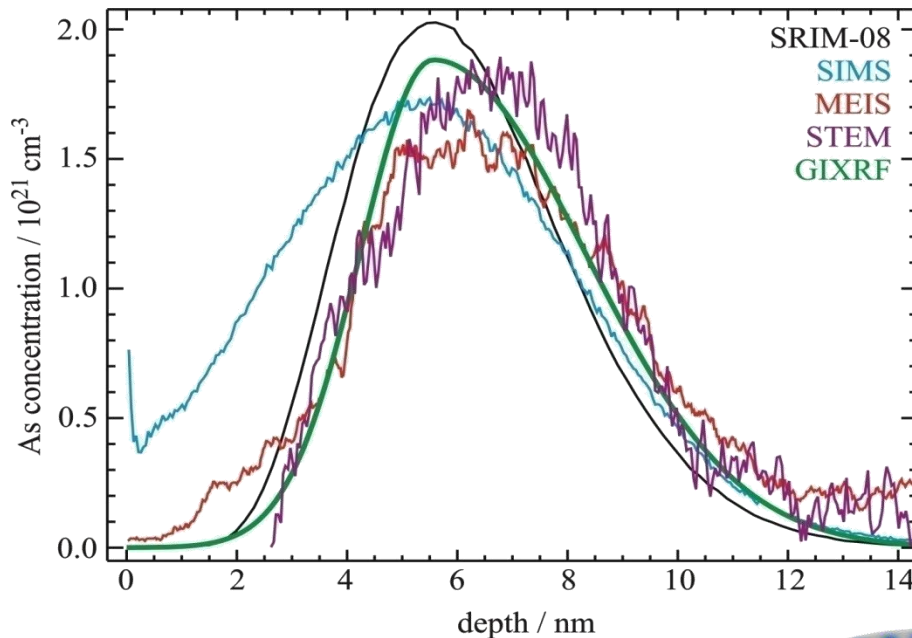
$$F_{Imp}(\theta) = G \int_0^{t_{max}} P_{Imp}(t) \cdot I_{XSW}(t, \theta, E_0) \cdot \left(e^{-\frac{t \rho \mu_{tot}(t)}{\sin \theta_{det}}} \right) dt$$

P. Hönicke

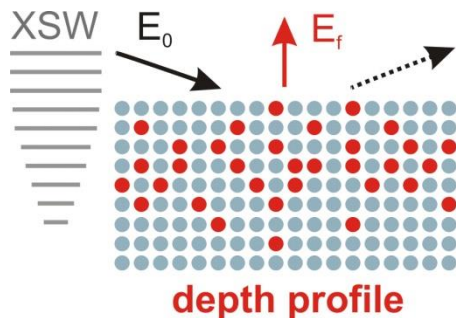
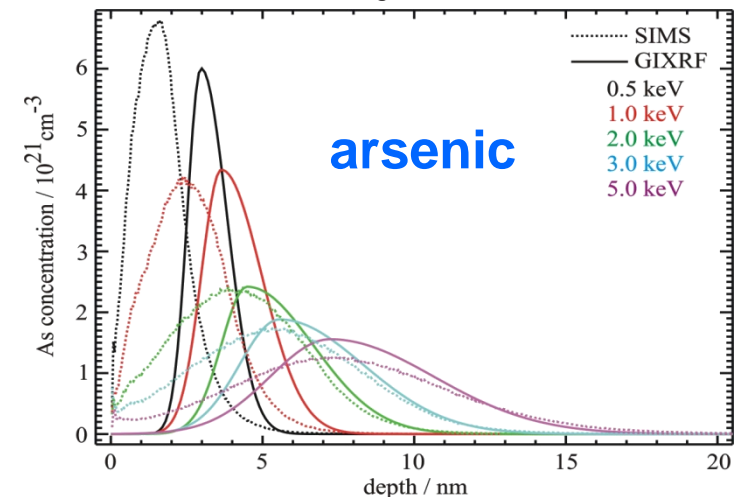
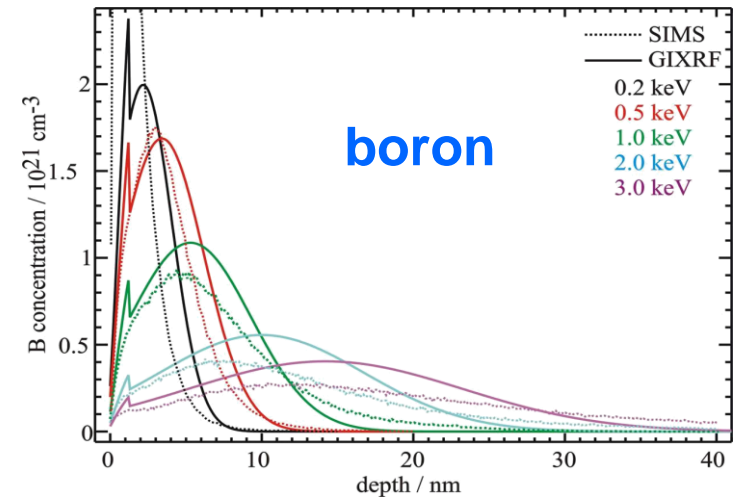
Anal. Bioanal. Chem. **396**, 2825 (2010)

GIXRF analysis of B and As implantation profiles

Comparison of GIXRF results on arsenic samples to SIMS, MEIS and STEM



Comparison of GIXRF results to SIMS



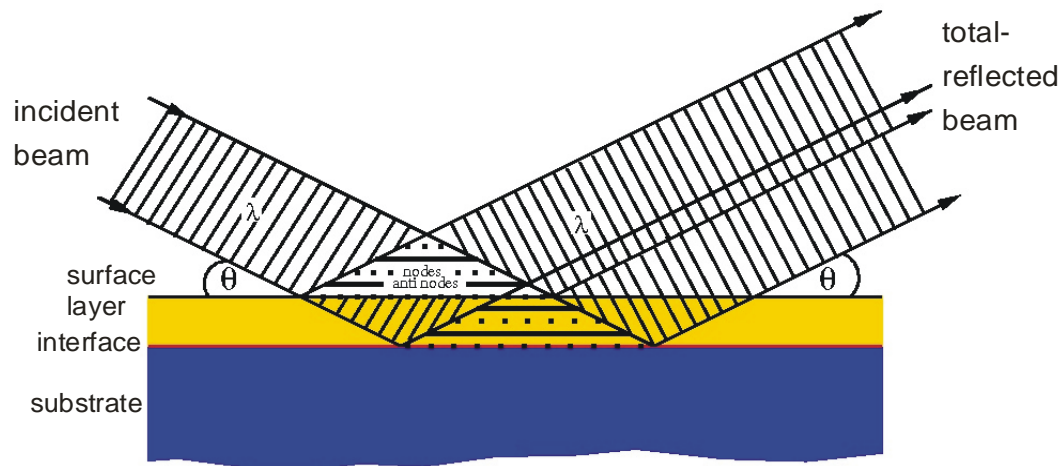
D. Giubertoni (FBK)

J. van den Berg (Univ. Salford)

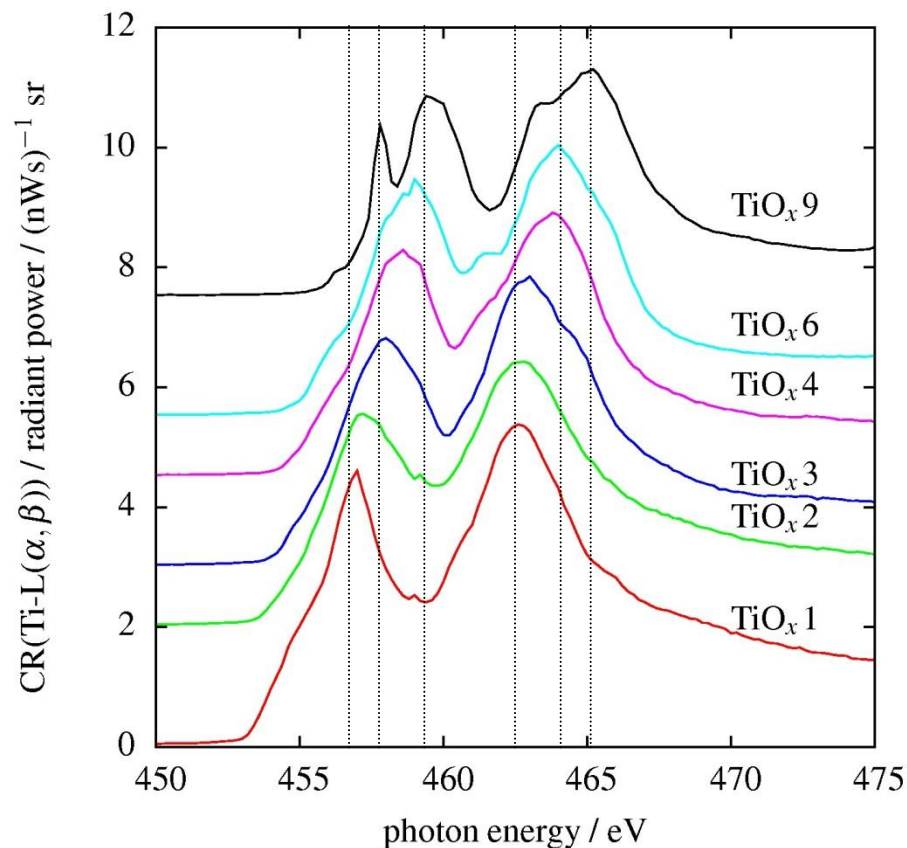
P. Hönicke

Anal. Bioanal. Chem. **396**, 2825 (2010)

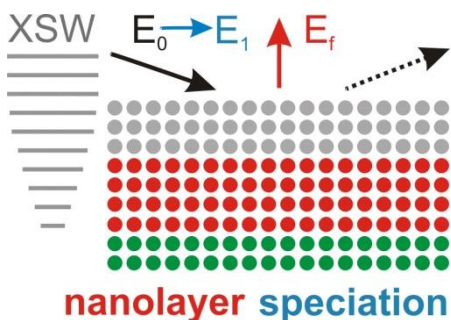
Speciation of buried nanolayers by GIXRF-NEXAFS



GIXRF-NEXAFS at the Ti-L_{iii,ii} edges



- composition and speciation of buried nanolayers
- higher information depth (>> 5nm) than XPS
- parallel variation of incident angle and photon energy



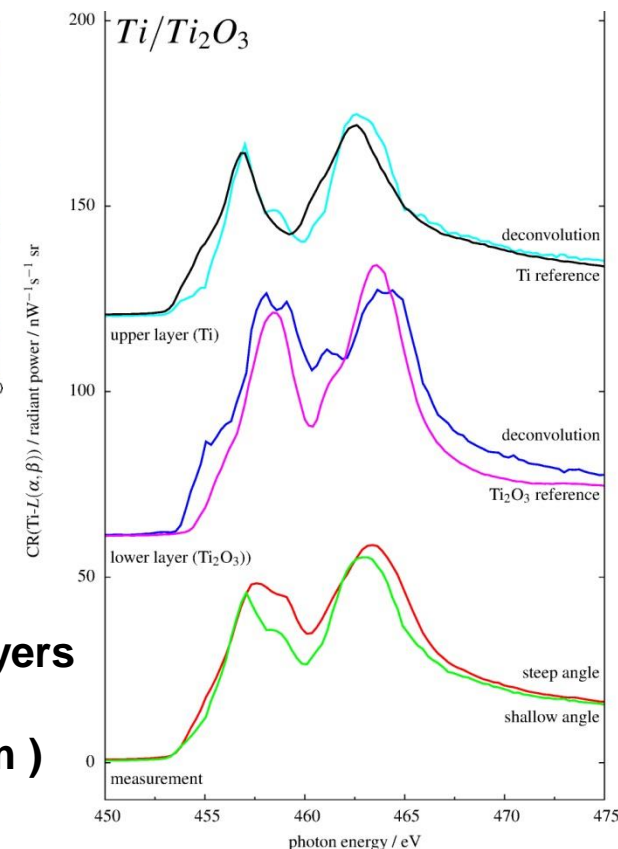
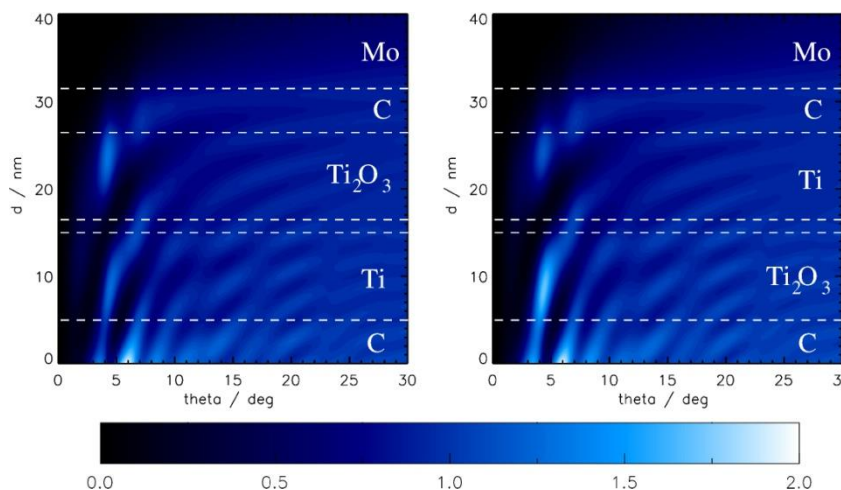
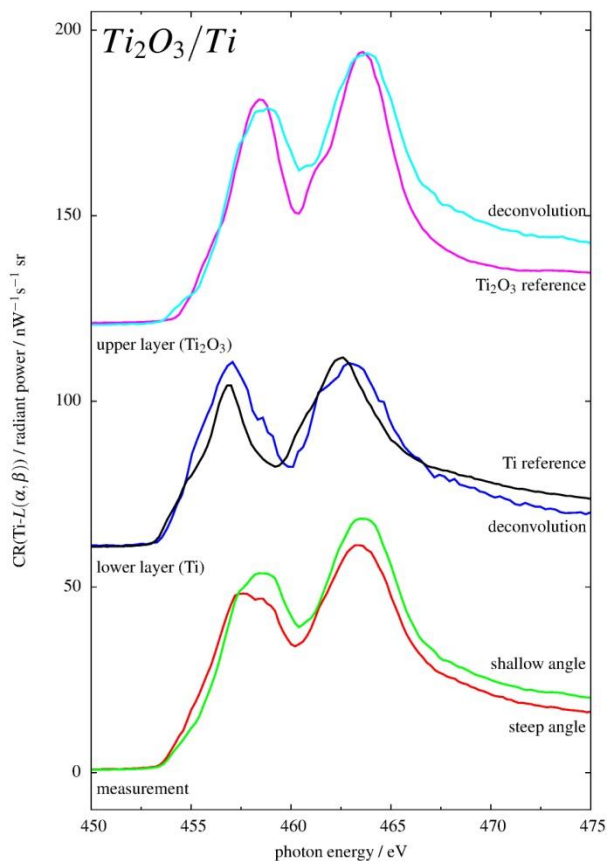
B. Pollakowski

Phys. Rev. B **77**, 235408 (2008)

Anal. Chem. **85**, 193 (2013)

speciation of buried Ti oxide nanolayers
(the degree of oxidation scales with indices)

Speciation depth profiling by GIXRF-NEXAFS

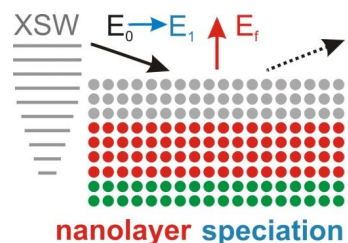


→ speciation of $Ti_{x_1}O_{y_1} / Ti_{x_2}O_{y_2}$ nanolayers

→ high information depth (up to 500 nm)

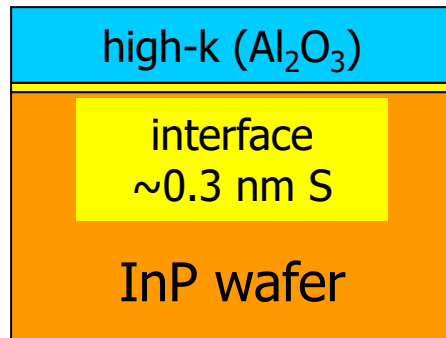
→ simultaneous variation of angle of

incidence and of the photon energy

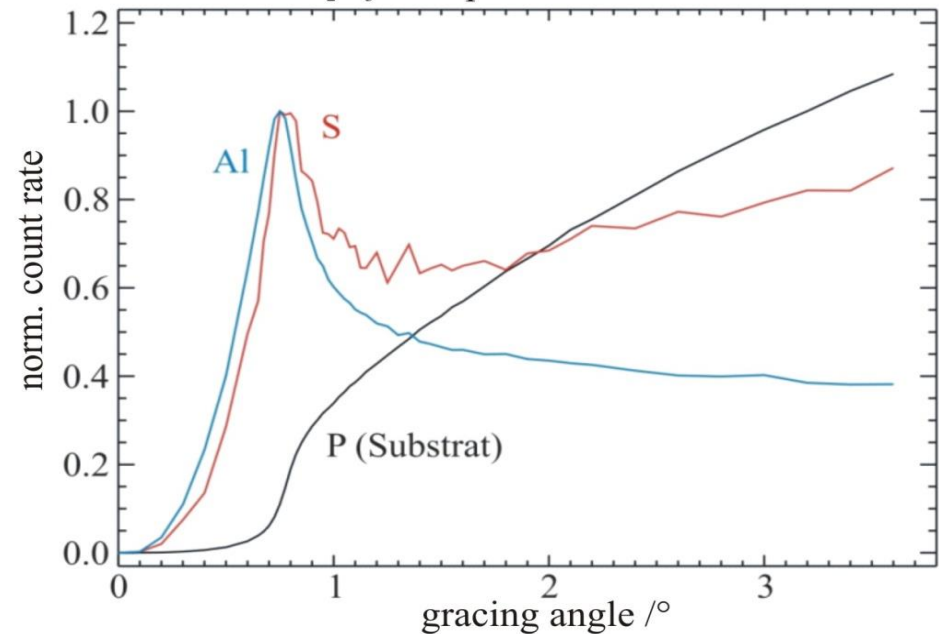


Quantitative characterization of nanoelectronics

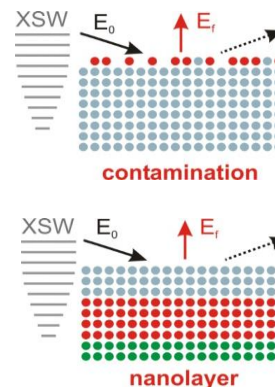
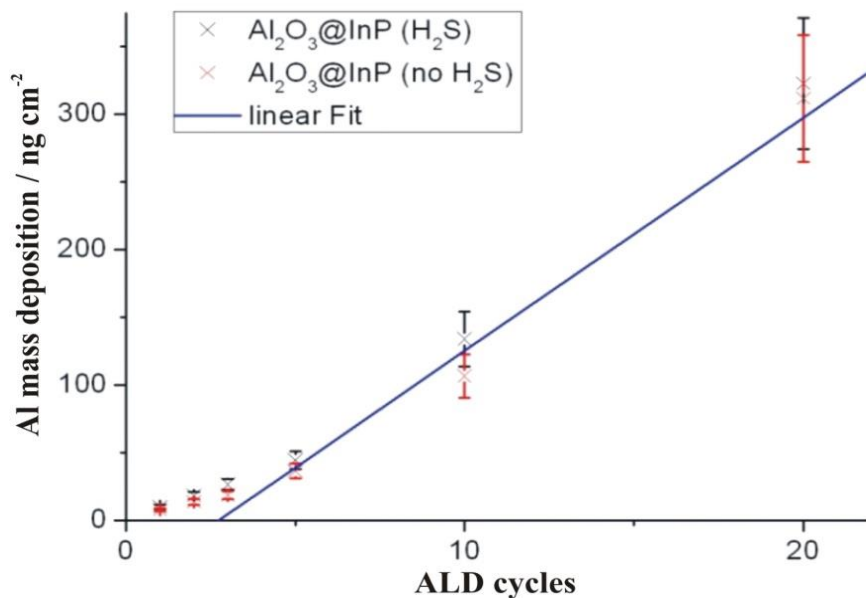
Optimization of high-k nanolayer fabrication



3 nm Al₂O₃ on S passivated INP substrate



Quantification of the ALD growth rate

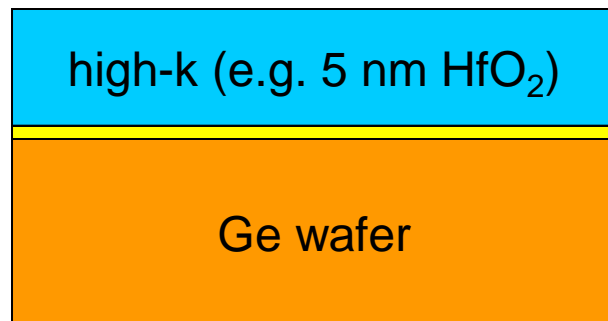
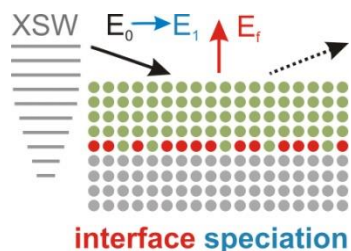
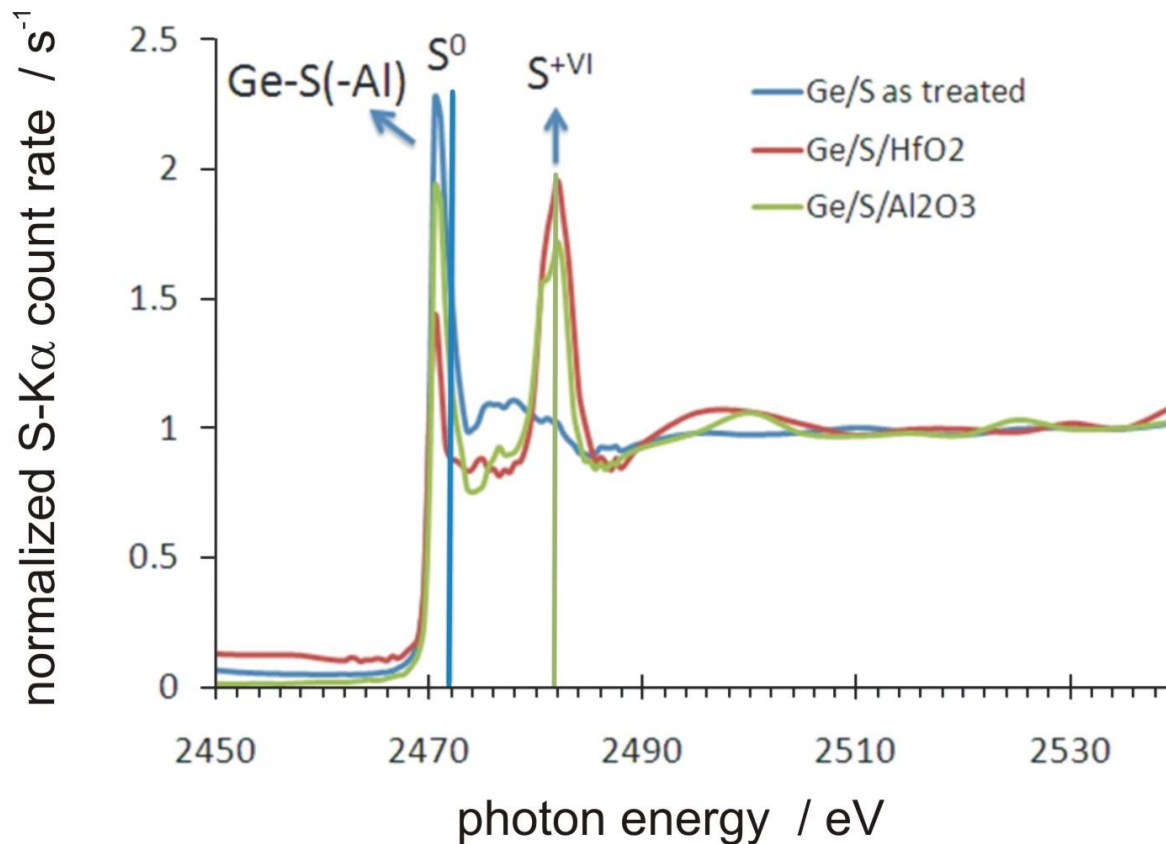


linear growth on S passivated InP substrate after the 3rd ALD cycle

J. Vac. Sci. Technol. A **30**, 01A127 (2012)

Quantitative interface characterization and speciation

XAFS speciation of the S passivated interface as treated and for two high k cap layer



passivated interface
(S monolayer ~0.3 nm)

M.Müller

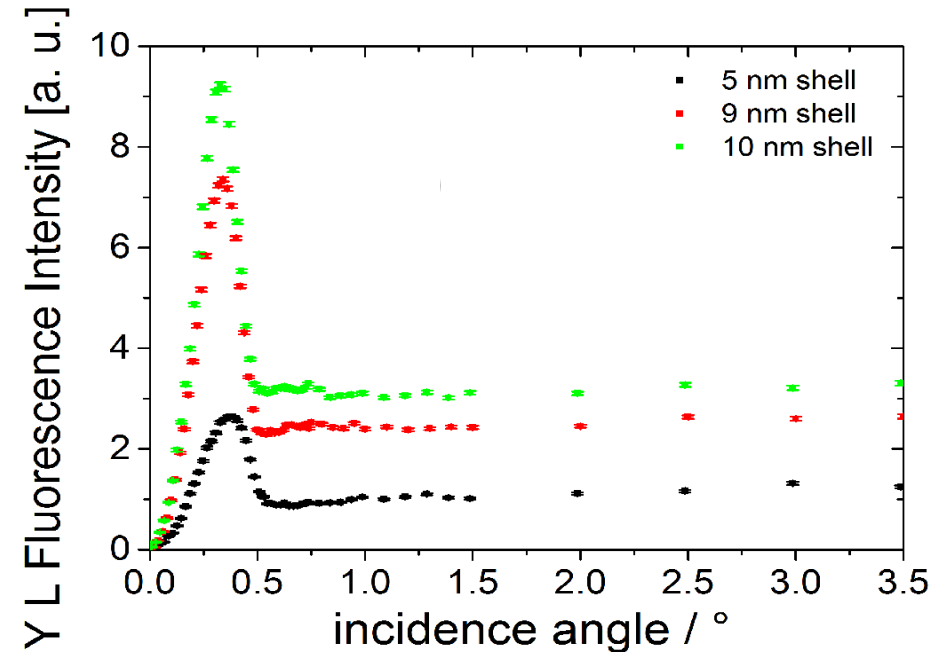
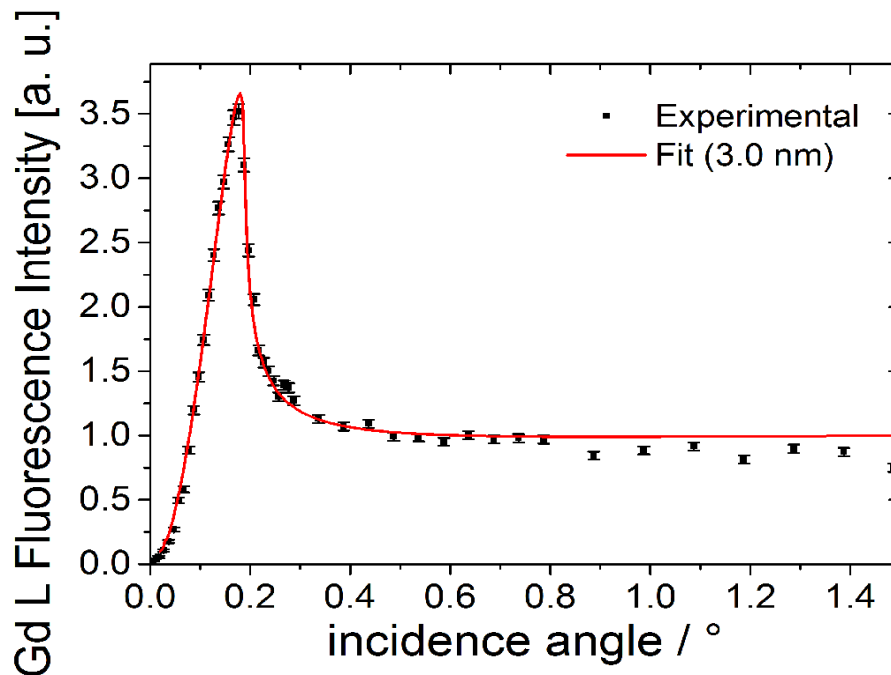
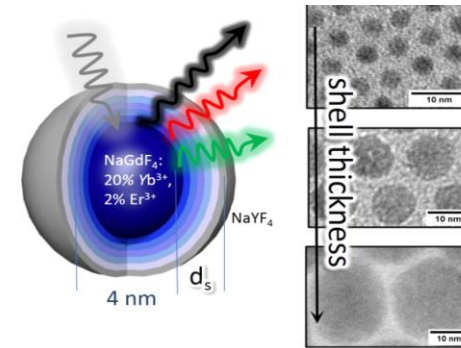
J. Electrochem. Soc. **158**, H1090 (2011)



GIXRF based characterization of nanostructures - nanoparticles -

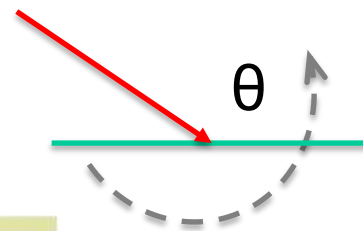
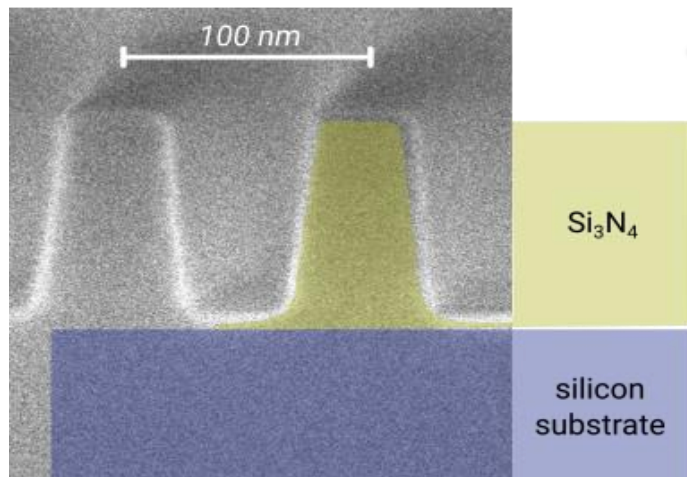
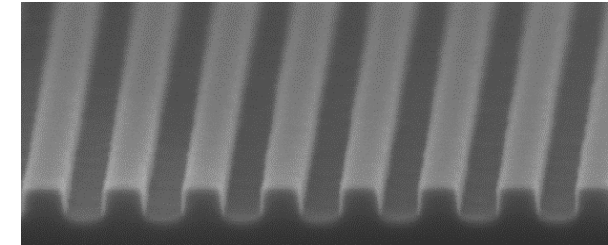
• Core-shell nanoparticle depositions on Si

- Determination of deposition densities using reference-free quantification
- modeling of GIXRF data to determine e.g. core size

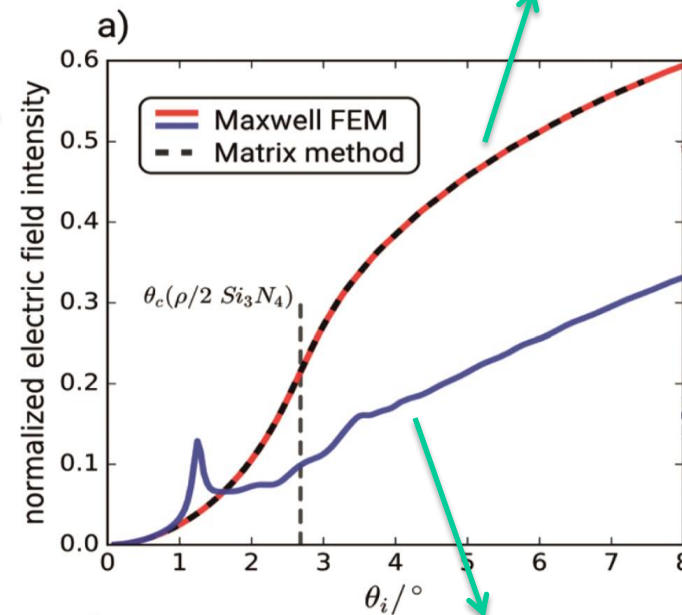


GIXRF based characterization of nanostructures - well-ordered 2D nanostructures -

- Si_3N_4 patterned grating on Si
 - grating with pitch, height and width
 - GIXRF at 520 eV to detect nitrogen fluorescence



Effective density layer calc.

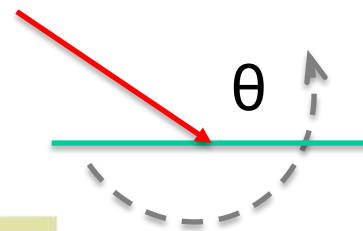
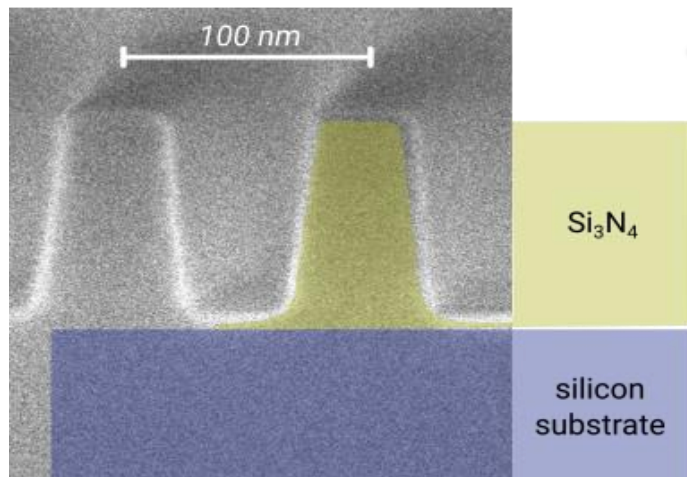
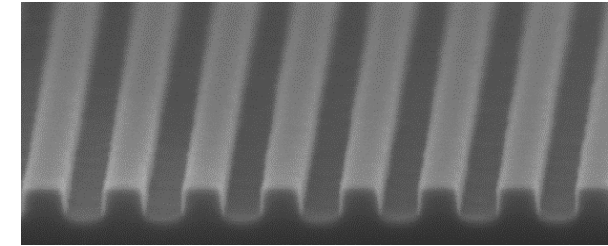


FEM calc. of real structure

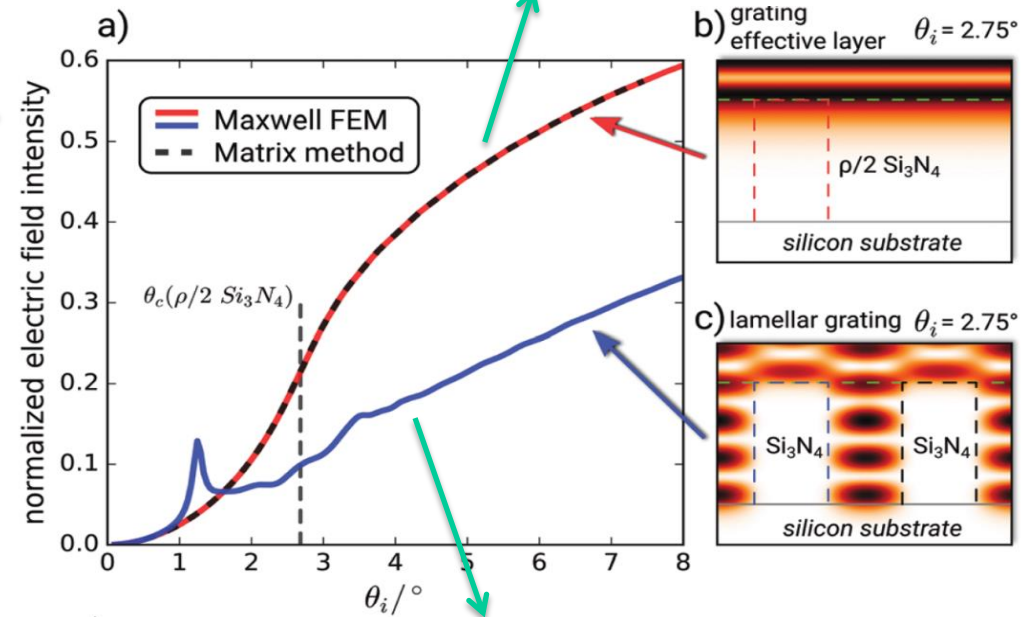
GIXRF based characterization of nanostructures

- well-ordered 2D nanostructures -

- Si_3N_4 patterned grating on Si
 - grating with pitch, height and width
 - GIXRF at 520 eV to detect nitrogen fluorescence



Effective density layer calc.

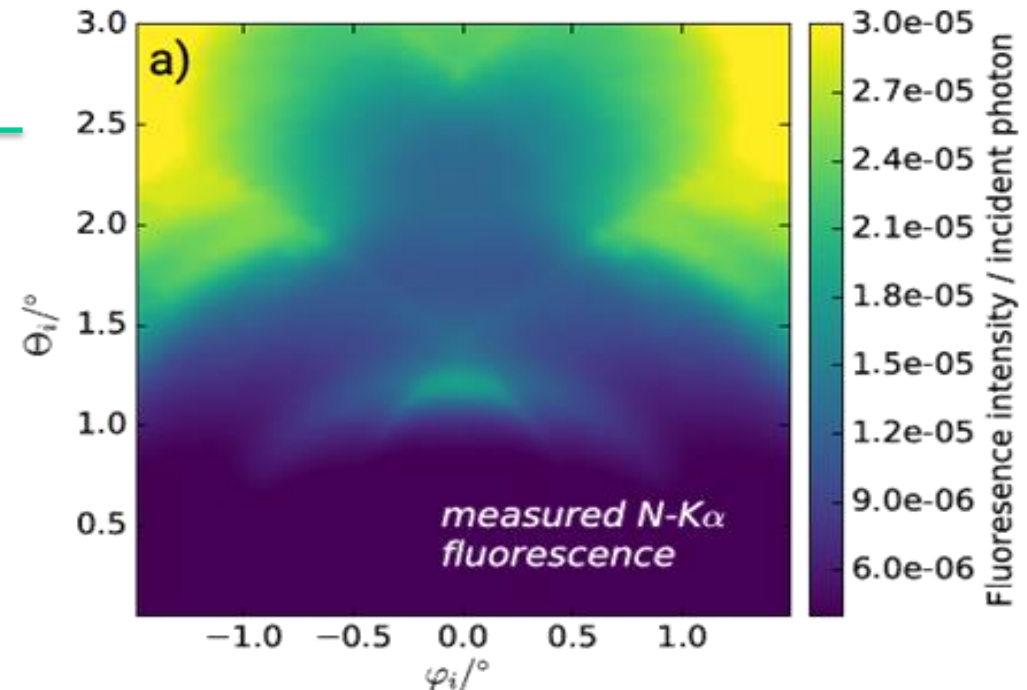
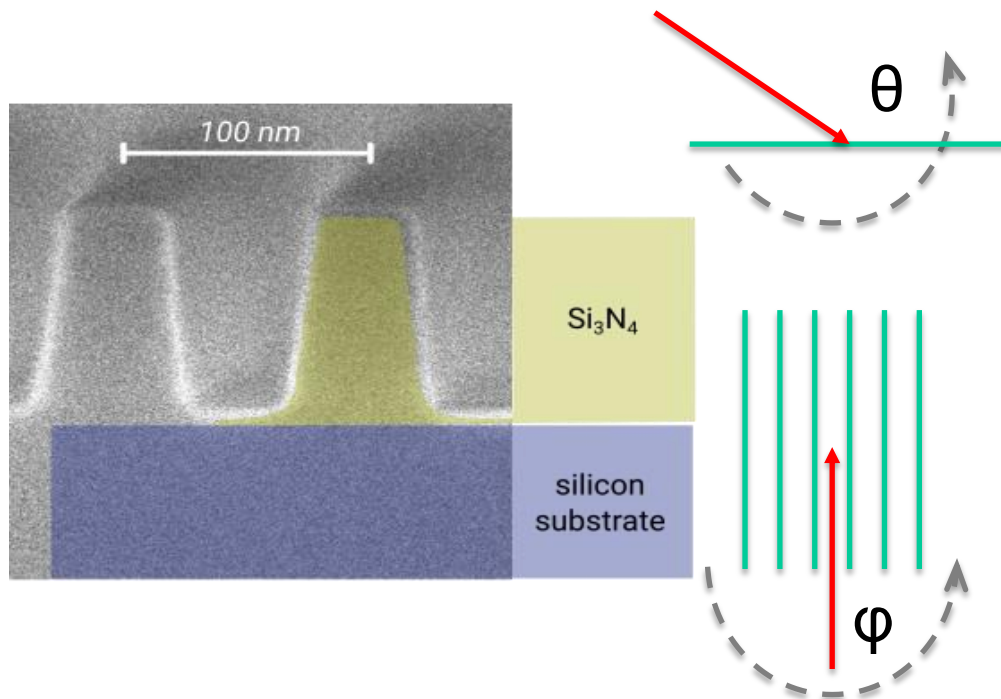
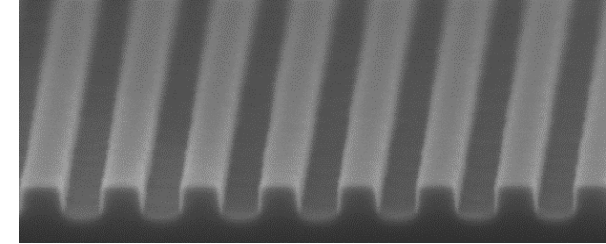


FEM calc. of real structure

GIXRF based characterization of nanostructures - well-ordered 2D nanostructures -

- **Si₃N₄ patterned grating on Si**

- grating with pitch, height and width
- GIXRF at 520 eV to detect nitrogen fluorescence
- θ (beam and surface) and φ (beam and grating) are varied



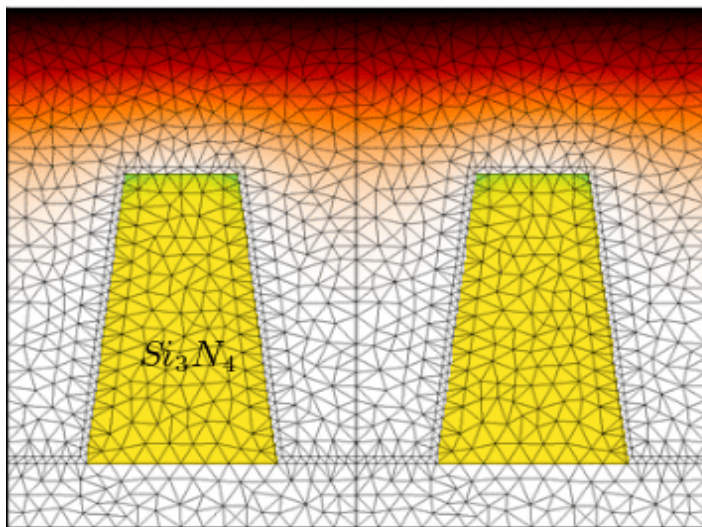
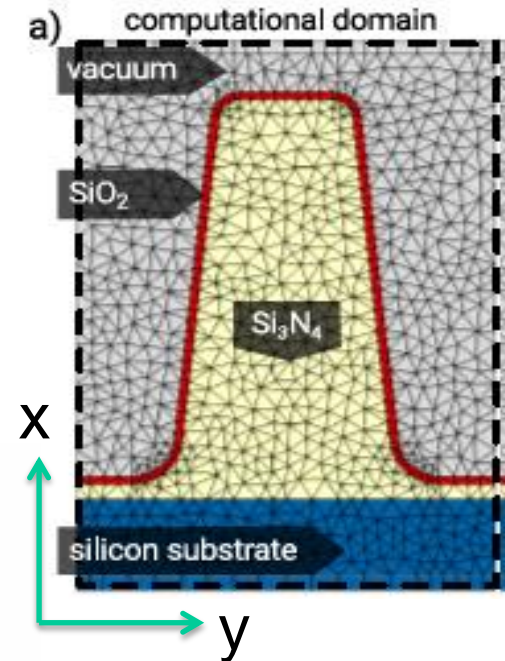
GIXRF based characterization of nanostructures - well-ordered 2D nanostructures -

model parameters

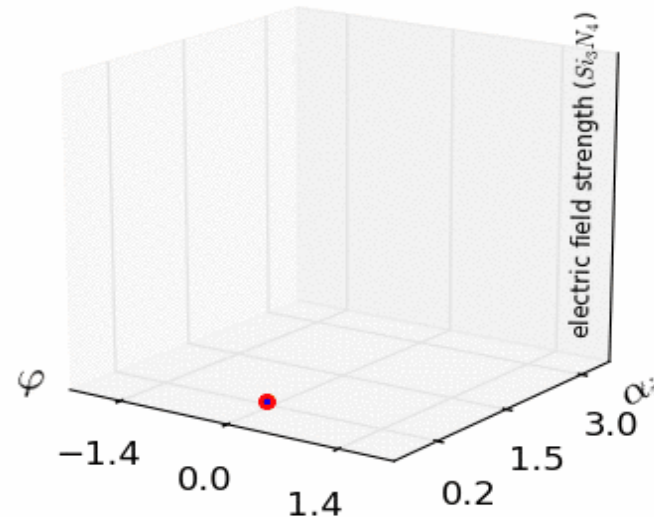
- width, height and pitch
- oxide thickness and groove edge residue

$$\frac{4\pi \sin \theta_i}{\Omega} \frac{F(\theta_i, E_i)}{N_0 \epsilon E_f} = \frac{\text{FP's}}{\sum dx} \cdot \frac{\text{Electric field int.}}{\sum_x \sum_y |E(x, y)|^2 \cdot \exp[-\rho \mu_{E_i} y_{dis}]} \cdot \text{Atten. correction}$$

Norm. fluorescence



$\alpha_i = 0.1^\circ$
 $\varphi = 0.0^\circ$



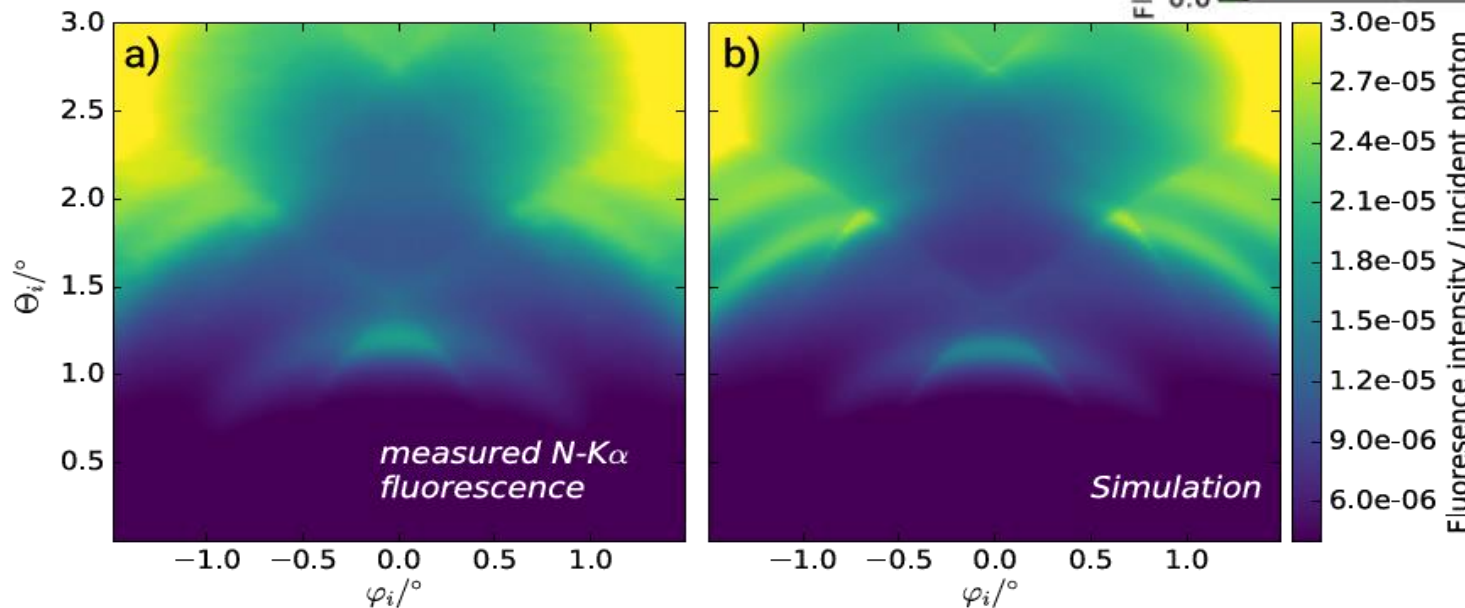
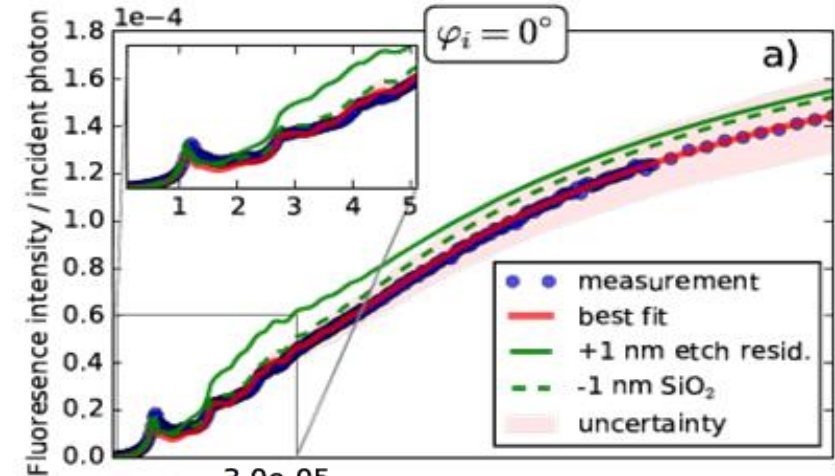
JCMwave

3D Maxwell Solver

GIXRF based characterization of nanostructures - well-ordered 2D nanostructures -

• Results Si_3N_4 grating

- Very sensitive for deviations of etch residue or oxide thickness
- Determination of dimensional properties and elemental distributions



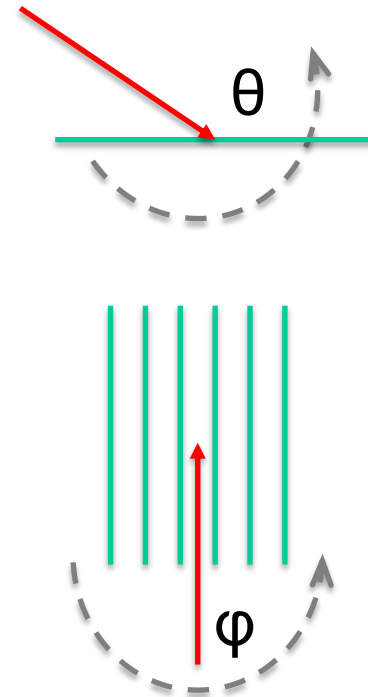
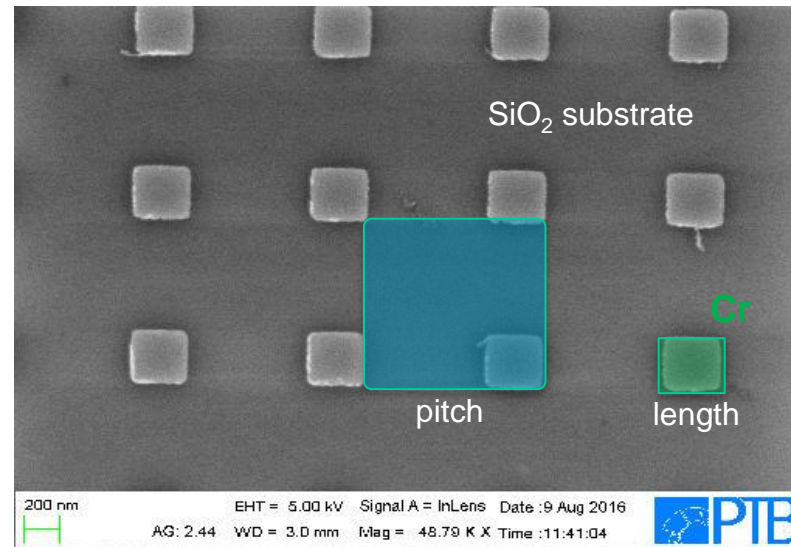
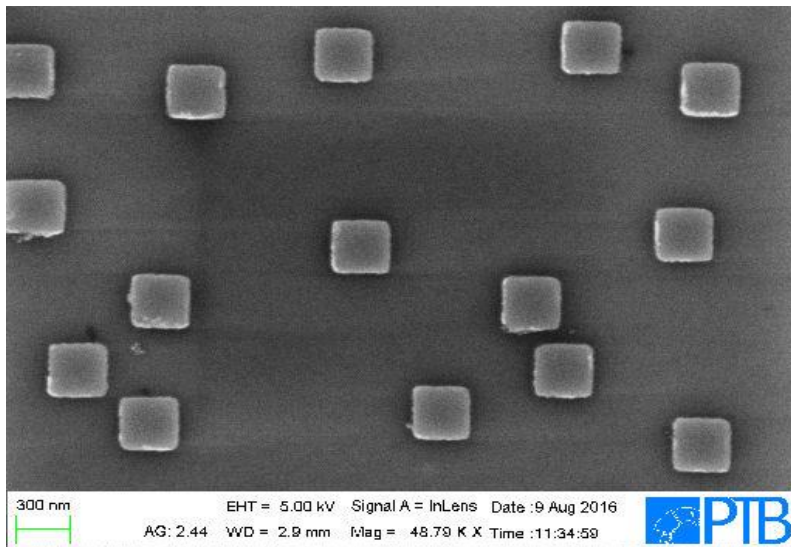
JCMwave

3D Maxwell Solver

GIXRF based characterization of nanostructures

- 3D nanostructures -

- Cr rectangular nanostructures on SiO₂: 300x300x20 nm³ blocks
 - 1000 nm pitch and 300 nm width
 - ordered array and non-ordered patterns (identical average pitch)
 - GIXRF experiments performed with varying phi excitation



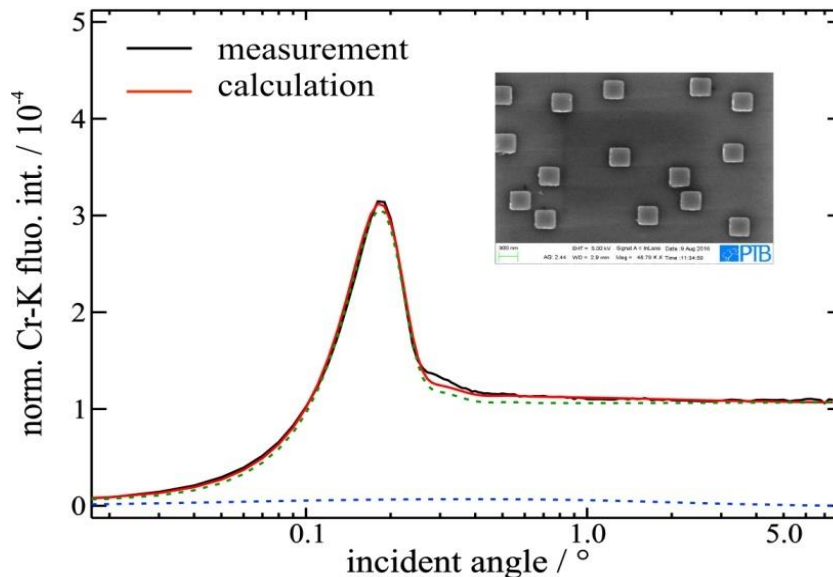
GIXRF based characterization of nanostructures

- 3D nanostructures -

- Cr rectangular nanostructures on SiO₂: 300 x 300 x 20 nm³ blocks

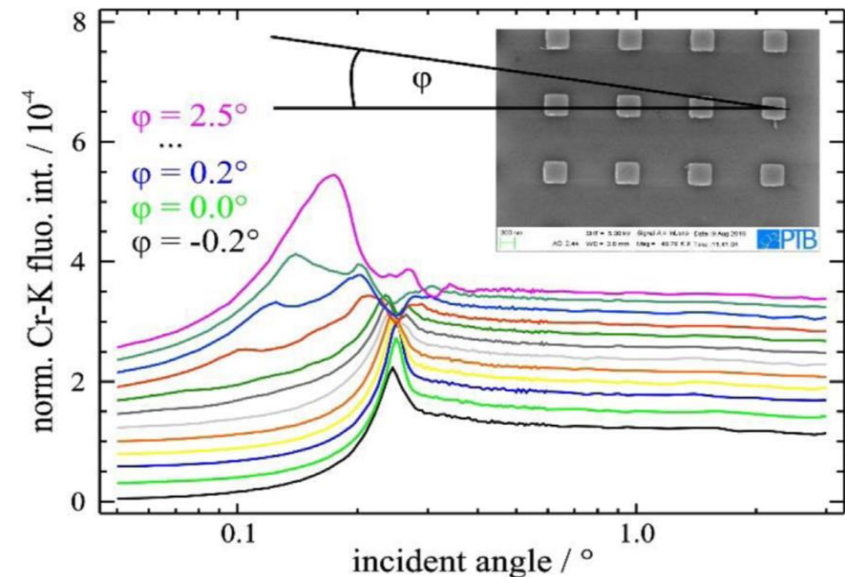
Non-ordered pattern:

- no phi dependence of the signal
- modeling of GIXRF based on effective density layer



Ordered pattern:

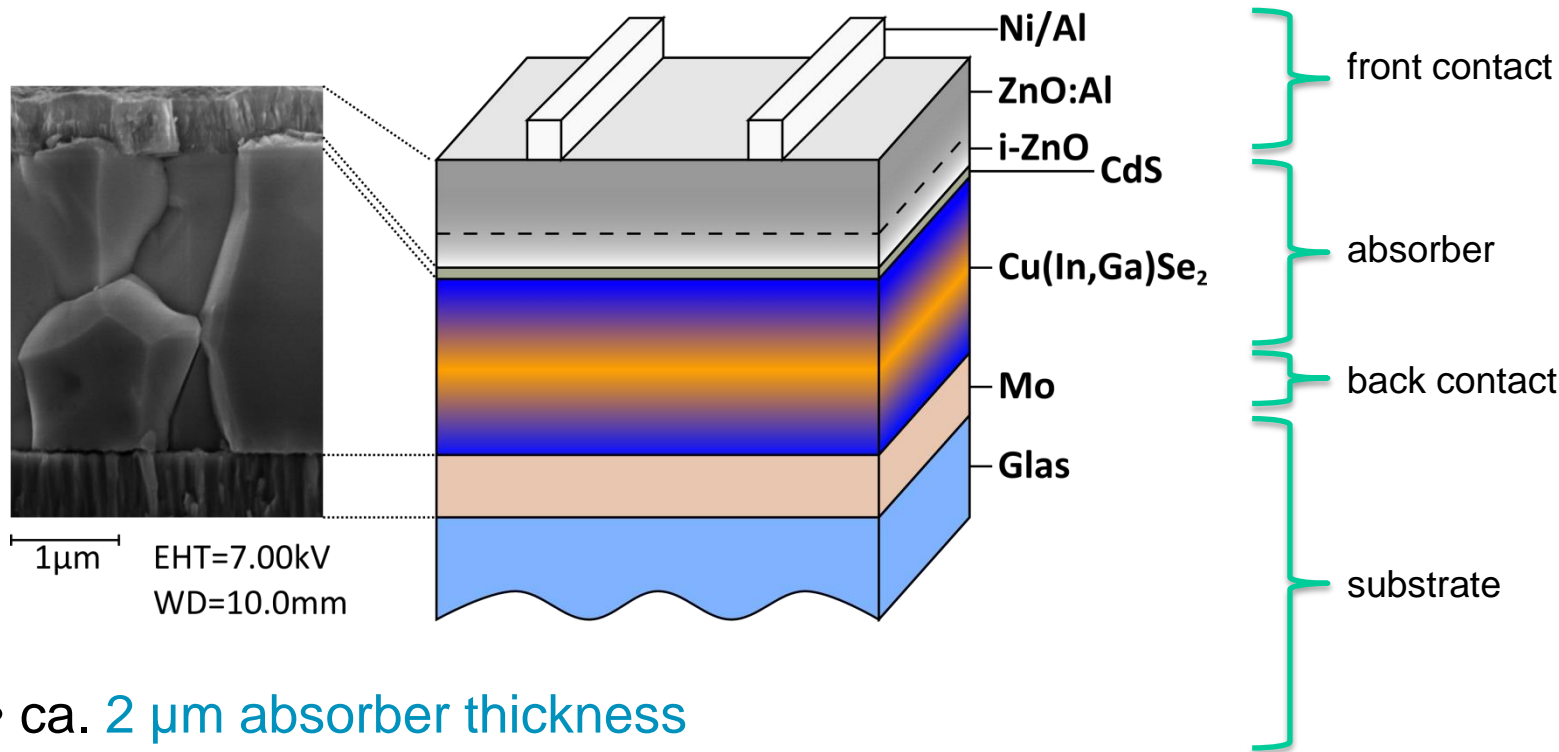
- Strong phi dependence
- FEM based modeling is computationally challenging



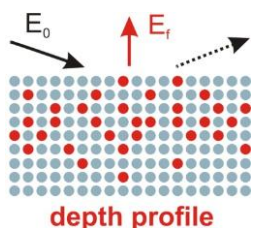
	SEM	GIXRF
length / nm	295 ± 12	288 ± 29
pitch / nm	992 ± 41	996 ± 99

Elemental depth profiling of CIGS photovoltaics by GIXRF using calibrated instrumentation

Cu(In,Ga)Se₂ absorber for thin film solar cells



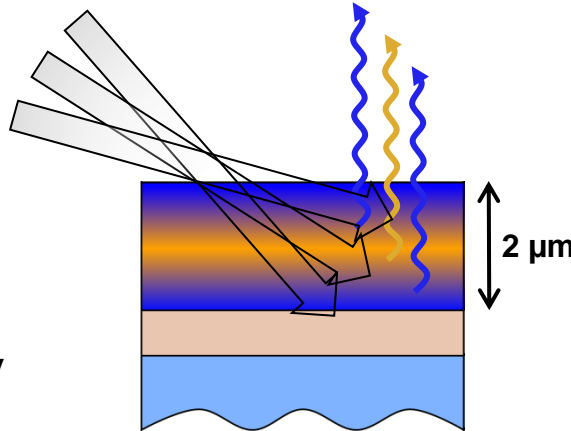
- ca. 2 μm absorber thickness
- inhomogeneous element depth distribution of In and Ga influences the efficiency



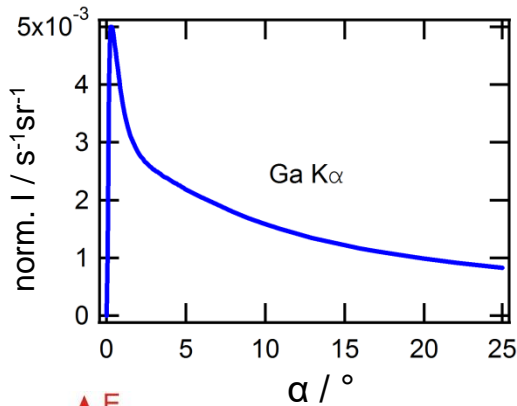
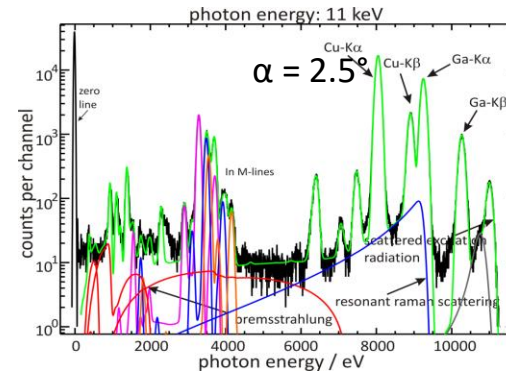
Elemental depth profiling of CIGS photovoltaics by GIXRF using calibrated instrumentation

Increasing information depth with increasing incidence angle

Fluorescence intensity in dependence of the angle of incidence



XRF-spectrum

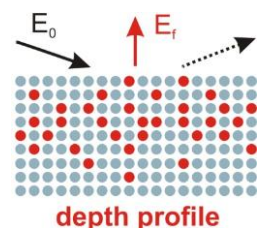
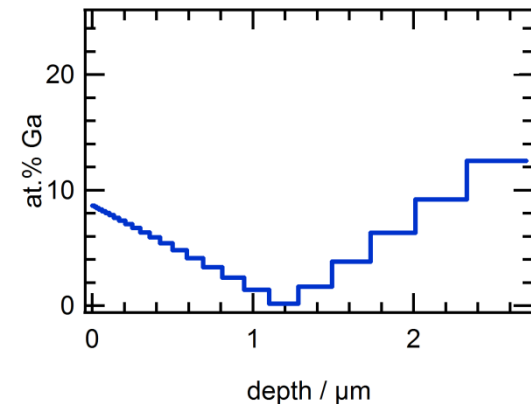


GIXRF

Non-destructive access to the elemental depth profile

Fundamental parameter-based quantification

Elemental depth profile



Comparison of in-depth resolving techniques

Non-destructive traceable technique:
reference-free XRF analysis

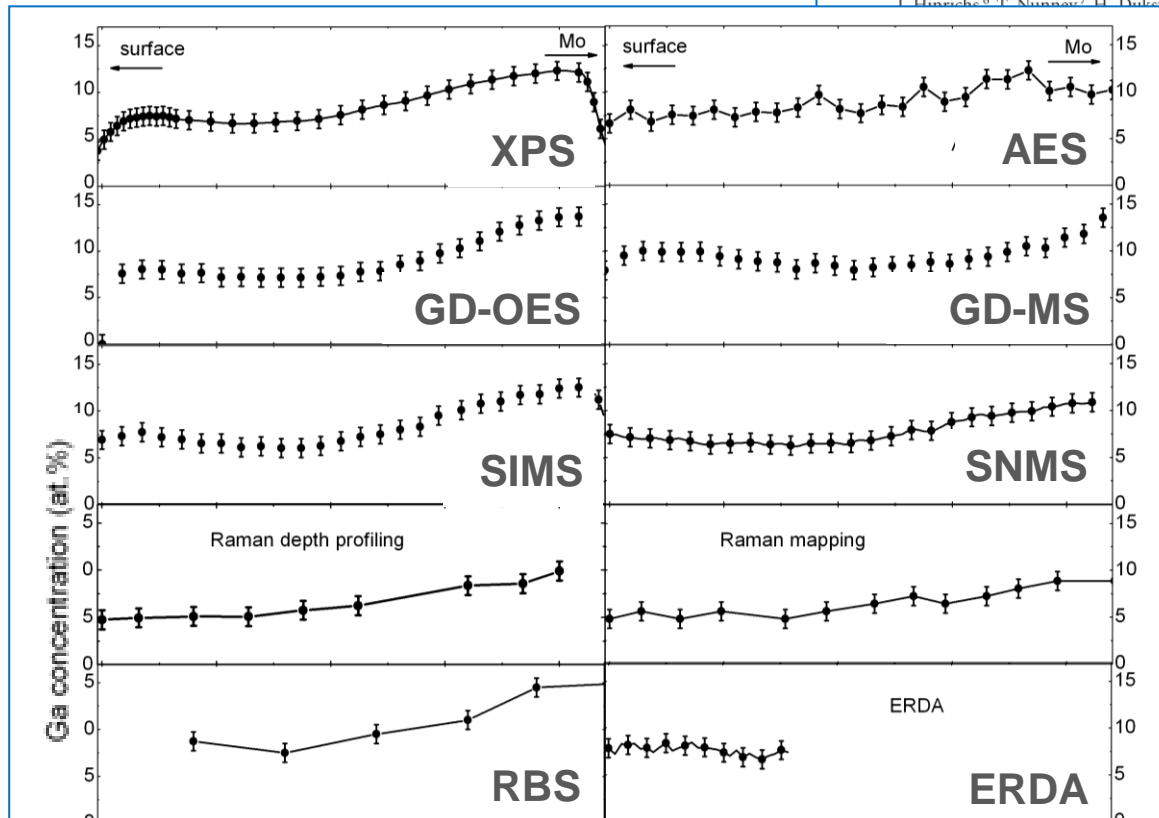
Microsc. Microanal. 17, 728–751, 2011
doi:10.1017/S1431927611000523

Microscopy AND
Microanalysis

© MICROSCOPY SOCIETY OF AMERICA 2011

Comprehensive Comparison of Various Techniques for the Analysis of Elemental Distributions in Thin Films

D. Abou-Ras,^{1,*} R. Caballero,¹ C.-H. Fischer,¹ C.A. Kaufmann,¹ I. Lauermann,¹ R. Mainz,¹
 H. Mönig,¹ A. Schöpke,¹ C. Stephan,¹ C. Streeck,¹ S. Schorr,² A. Eicke,³ M. Döbeli,⁴ B. Gade,⁵
 I. Hübsche,⁶ T. Nunnay,⁷ H. Dülster,⁸ V. Hoffmann,⁹ D. Klemm,⁹ V. Efimova,⁹ A. Bergmaier,¹⁰
 A.A. Rockett,¹¹ A. Perez-Rodriguez,^{13,14} J. Alvarez-Garcia,¹⁵
 P. Choi,¹⁷ M. Müller,¹⁸ F. Bertram,¹⁸ J. Christen,¹⁸
 Ilac,¹⁹ and I. Kötschau²⁰



- more than 20 analytical techniques
- On sections of a laterally homogeneous sample
- Quantitative differences larger than uncertainties of single techniques
- Most methods require a calibration sample



Elemental depth profiling of CIGS photovoltaics by GIXRF using calibrated instrumentation

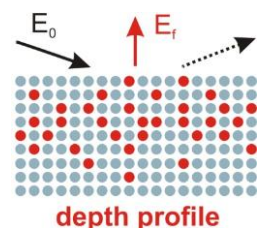
BIPM pilot-study CCQM-P140:

Quantitative surface analysis of multi-element alloy films

SURFACE ANALYSIS

Measurement of atomic fractions in $\text{Cu}(\text{In,Ga})\text{Se}_2$ Films

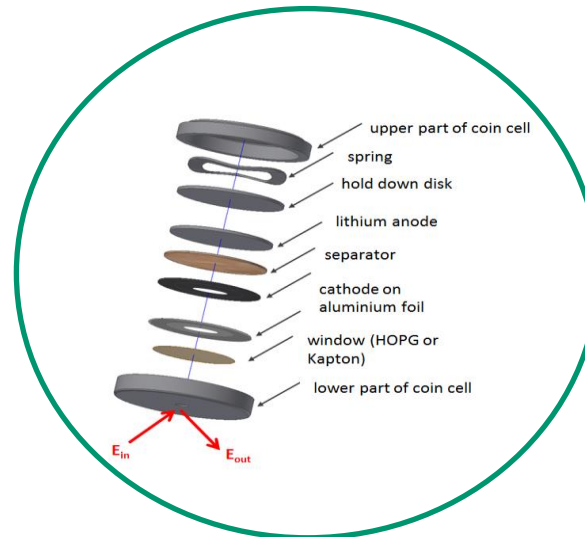
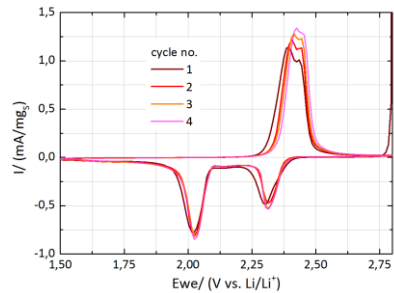
Composition / at. %	Certified values  Korea Research Institute of Standards and Science	Reference-free GIXRF 
Cu	23.8 ± 0.6	24.0 ± 1.3
In	19.1 ± 0.6	19.3 ± 1.1
Ga	6.6 ± 0.3	6.3 ± 0.4
Se	50.6 ± 1.5	50.4 ± 2.8
d / μm	ca. 2	2.06 ± 0.09



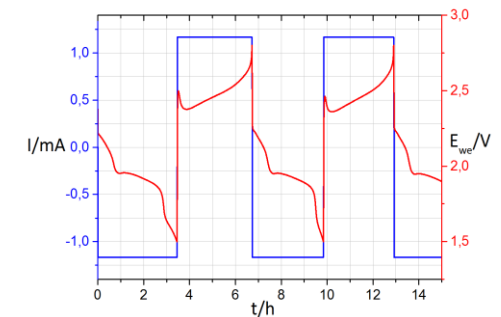
In-situ / operando battery characterization by means of Near-Edge X-ray Absorption Fine Structure (NEXAFS)

combination of morphologic, structural, and performance probing investigation to reveal a most complete understanding of the battery degradation mechanism

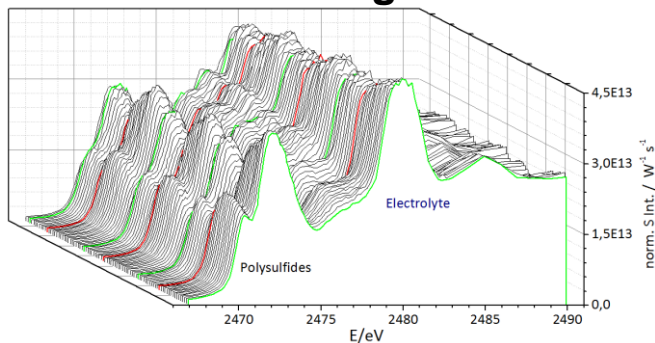
cyclovoltammetry



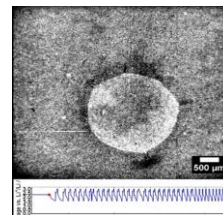
electrochemical characterization



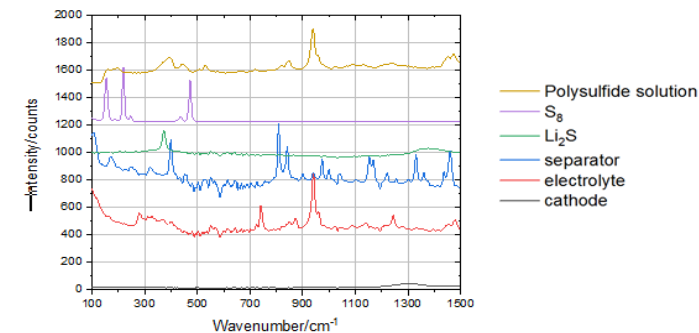
operando NEXAFS at the sulfur K edge



operando X-ray radiography (HZB Wannsee)



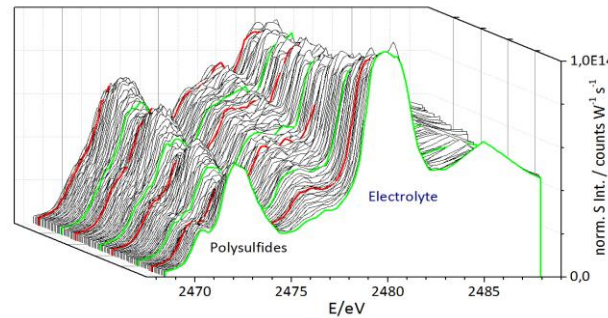
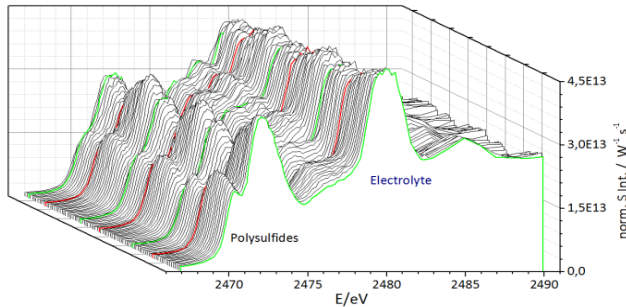
operando Raman spectroscopy (IFP Dresden)



Operando NEXAFS investigations of Li-S batteries from 2 sides

cathode side

anode side



operando NEXAFS spectra



spectral deconvolution



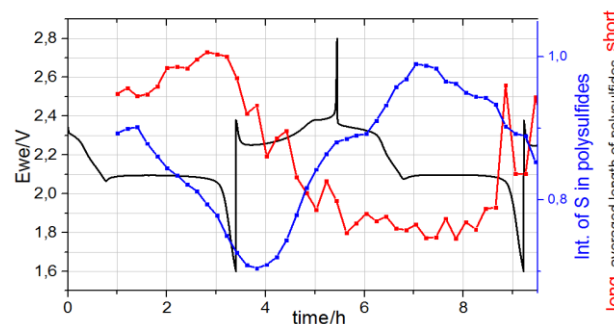
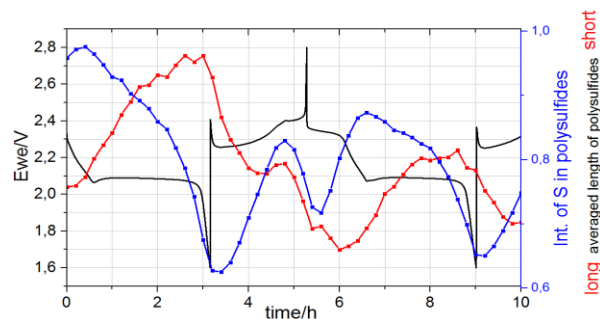
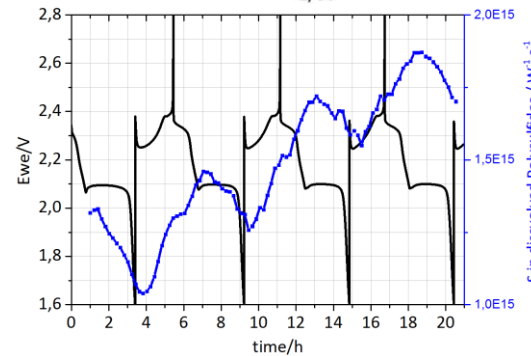
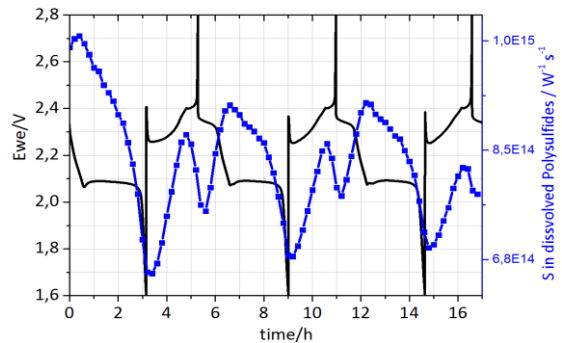
Variation of the polysulfide concentration across three charging/discharging cycles



Deduction of the length of polysulfide chain lengths

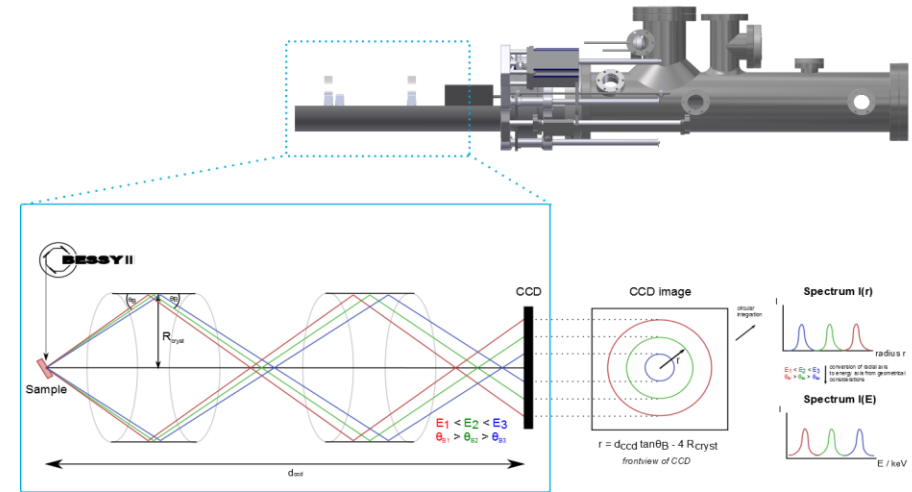


Better understanding of the polysulfide shuttle in LiS batteries



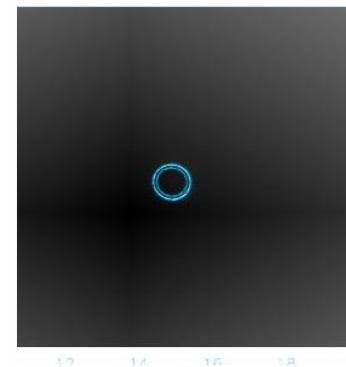
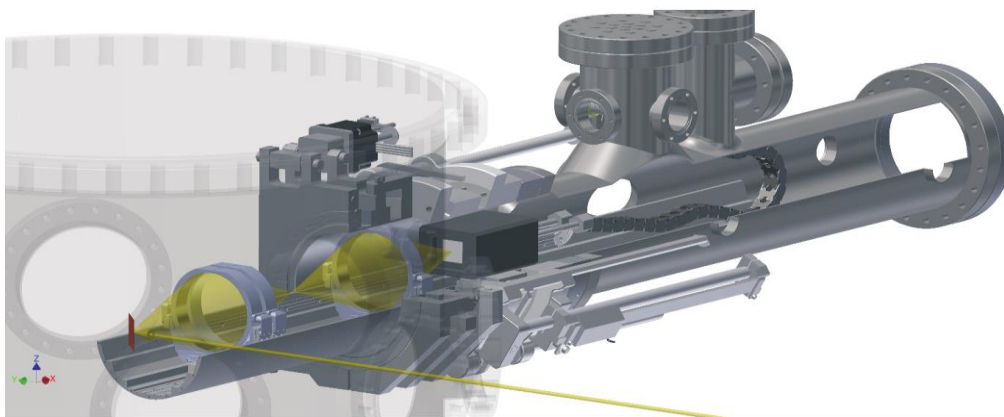
Compact von Hamos spectrometer for high-resolution x-ray emission – FP determination and chem. speciation

- Commissioning of the new spectrometer and development of CCD data analysis software
- Robust calibration concepts for reference-free XRS and XES

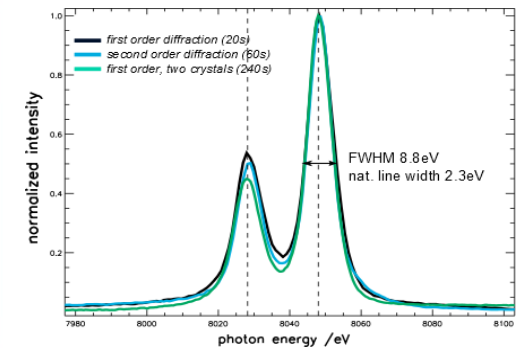


2) schematical arrangement and principle

1) Side view of the spectrometer



3) recorded CCD data

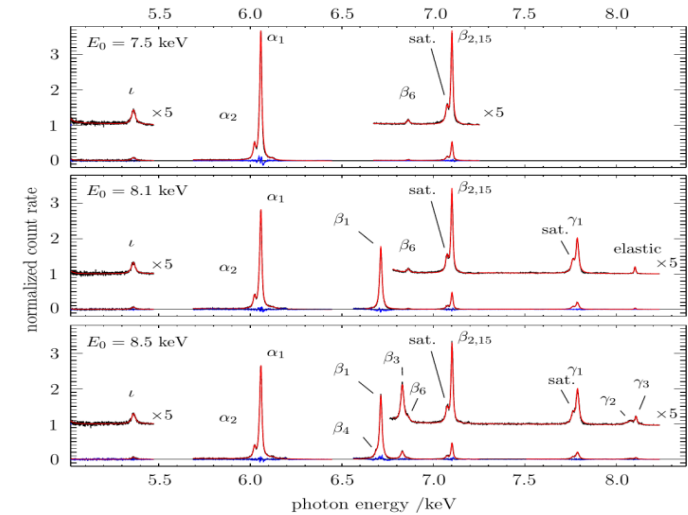


4) spectra deduced from CCD data

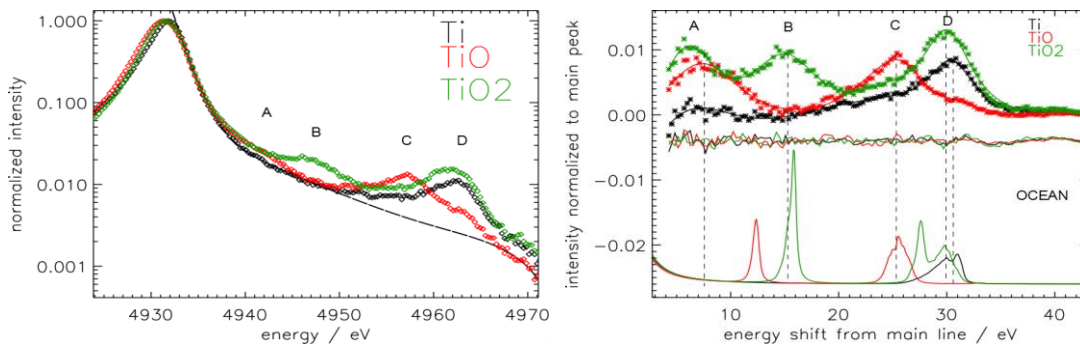
Compact von Hamos spectrometer for high-resolution x-ray emission – FP determination and chem. speciation

Fields of application

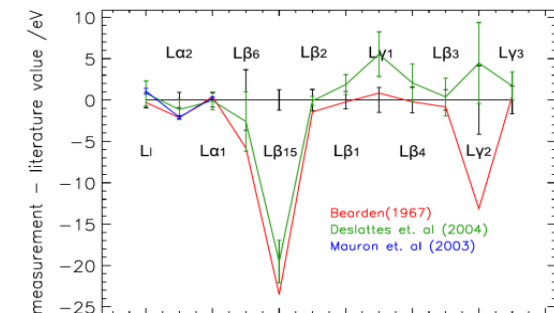
- Chemical speciation (reference-free determination of species mass depositions)
- Determination of x-ray fundamental parameters (FP) using the calibration
 - line energies
 - line intensities (transition and CK propabilities)



6) gadolinium L emission spectra for subshell selective photon excitations



5) Valence-to-Core XES of titanium compounds and comparison to calculations (OCEAN) in cooperation with the US NMI NIST



7) Comparison of measured gadolinium L line energies with NIST reference data

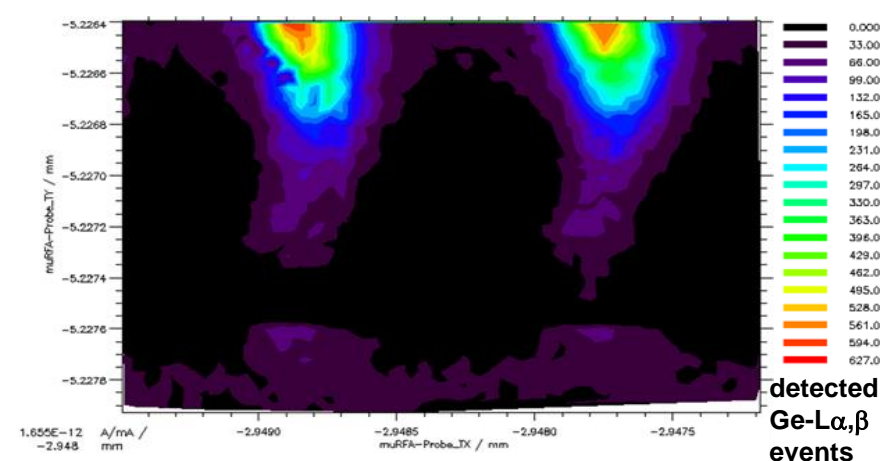
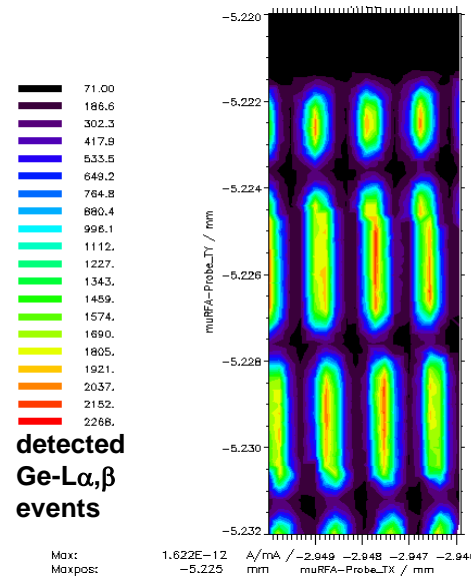
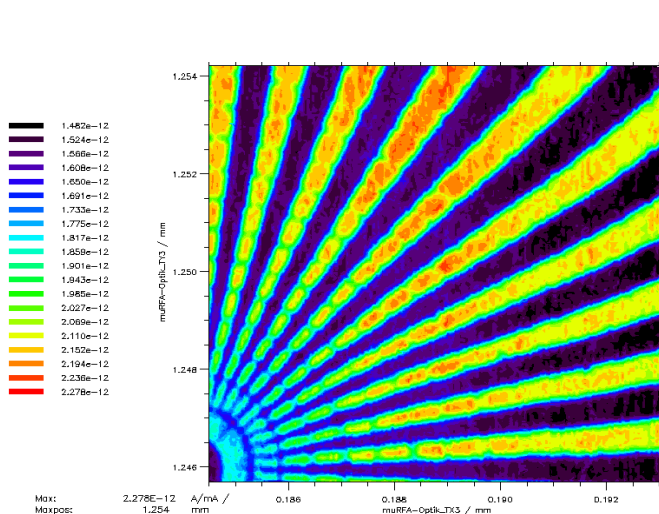
Traceable X-ray fluorescence analysis with spatial resolutions in the 100 nm range

Vibration reduced approach in existing XRF instrumentation of PTB for nanoanalytics by means of a joint optics-sample platform

90 nm spatial resolution

450 nm spatial resolution

140 nm spatial resolution



Reference-free XRF at the end zones of two 150 nm wide SiGe structures (100 μm pinhole at the PGM focal plane)

photon energy of 1500 eV

Transmittance of a Siemens star at the PGM-U49 beamline (50 μm pinhole at PGM focus)

1st reference-free XRF analysis of 150 nm wide, 3 μm long SiGe structures

AEROMET

Aerosol metrology for atmospheric science and air quality



Dimensional metrology

AEROMETPROJECT.COM

Analytical metrology

CPC calibration

In-field aerosol sampler

**SIZE,
NUMBER,
MASS**

Test aerosol generation

Comparison of aerosol instruments at outlets 1, 2 and 3

MPSS calibration

Reference test aerosol, d_T

displayed particle size, d_M

Reference particles

Field applicable XRF

COMPOSITION

New ICP-QQQ-MS

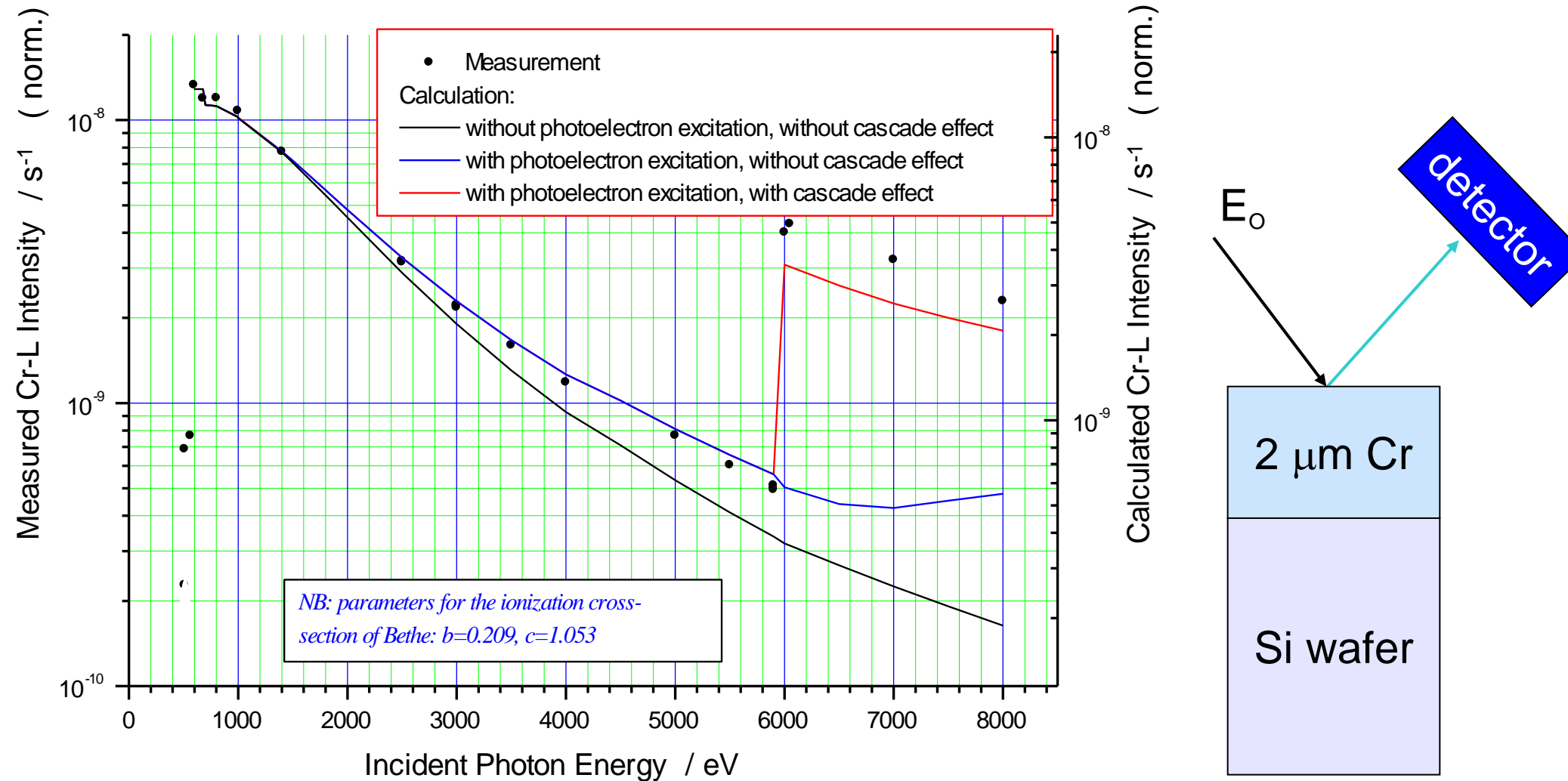
Traceable SR-GIXRF

Mixing chamber MPSS calibration

New ICP-QQQ-MS Traceable SR-GIXRF



photoelectron and cascade effects: Cr L-lines



Summary

- Reference-free analysis of contamination on Si and of functionalized surfaces
- Quantitative characterization of nanostructured and gradient systems ($\sim 2 \mu\text{m}$)
- Depth profiling ($\sim 500 \text{ nm}$) and interfacial analysis of nanoscaled materials
- High-resolution x-ray emission spectrometer and battery operando NEXAFS
- Determinations of atomic fundamental parameters (cross sections, yields, ...)

Further information on **EMRP ENG51, ENG53, IND07, IND56, NEW01, SIB03**



and **EMPIR 14IND01, 14IND07, 14IND12, 15HLT01, 16ENG03, 16ENG05, 16ENV07** at **EURAMET.org**

Acknowledgements: IMEC, KU Leuven, IPF, LETI, LNHB, HZB, NPL, IWS, AXO, MEMC, Numonyx, BAM, Technical Universities Berlin, Darmstadt, Dresden and Ilmenau, & industrial partners of PTB

E-MRS symposia ,Analytical Techniques for Precise Characterization of Nanomaterials' 2014 - 2020

International initiative on x-ray fundamental parameters

METHODOLOGICAL APPROACH

- Initiate new measurements taking advantage of technical improvements
- Perform similar measurements in different institutes to establish reliability and associated uncertainties of the experimental values
- Perform calculation for selected cases (use calculations for interpolations and validation purposes)
- Compare calculation to experiment
- Provide reliable practical tables to users

International initiative on x-ray fundamental parameters

Participants and events

- Active participation from :
 - 4 National Metrology Institutes
 - > 14 Research institutes
 - 10 Industrial companies
 - > 100 members
- 10 international workshops (2008 – 2018)
- 2018: Denver X-Ray Conference FP session
- 2019: FP workshop in Lisbon (see www.exsa.hu)

International initiative on x-ray fundamental parameters

International meetings and objectives:

www.EXSA.hu

1 st workshop LNE (M.-C. Lépy)	Oct. 2008	→ definition of expert groups
2 nd workshop PTB (B. Beckhoff)	May 2009	→ road map generation
3 rd workshop LNE (M.-C. Lépy)	Nov. 2010	→ project options
4 th workshop NIST (T. Jach)	July 2011	→ def. of new expert groups
at the EXRS2012 conference	June 2012	→ FP roadmap document online
5 th workshop PTB (B. Beckhoff)	Febr. 2013	→ new expert group meetings
6 th workshop NIMS (K. Sakurai)	Sept. 2013	→ dissemination of information
7 th workshop LNE (M.-C. Lépy)	Mar. 2014	→ road map updates by new EGs
8 th workshop UNL (J.-P. Santos)	Apr. 2015	→ road map updates by new EGs
9 th workshop UNL (Ch. Jeynes)	Oct. 2016	→ new FP roadmap discussion
10 th workshop PTB (B. Beckhoff)	Oct. 2017	→ new FP roadmap approved

International initiative on x-ray fundamental parameters

Tenth FP workshop - Round table discussion on FPs

Are there any **recommendations for the most reliable data bases ?**

- **ionisation cross sections**

(including sub-shell values)

– *best:* recent experiments

second-best: Scofield (Cullen) data

- **fluorescence yields and CK**

transition probabilities

– *best:* recent experiments, second-best: Krause data

- **line energies**

– *best:* recent experiments, second-best: NIST phys. ref. data

www.exsa.hu/fpi.php

International initiative on x-ray fundamental parameters

2nd FP roadmap document released December, 2017

Roadmap document on atomic Fundamental Parameters for X-ray methodologies

Version 2.0

December 2017

www.exsa.hu/news/wp-content/uploads/IIFP_Roadmap_V2.pdf

Contents

Introduction

Reports of expert groups:

Expert group 1: Project management and fund raising

Expert group 2: New experimental determinations and methodology

Expert group 3: Theory & codes – challenges: competent use and update of parameters

Expert group 4: Integration of new experimental as well as theoretical parameters into critically evaluated compilations

Expert group 5: Establishment of a common data base accessible to the public

www.exsa.hu/fpi.php